



Jatco

JATCO TECHNICAL REVIEW

No.24

CONTENTS

Preface

Technology for solving the dilemma between carbon neutrality and economic activity	1
Hiroyuki KAI	

Technical Reports

～ Mini Feature: Carbon Neutral ～

Development of Energy-Analysis Platform for Carbon Neutrality	3
Taichi KIMURA Shoji SUZUKI	
Masashi KOKAI Hitoshi WATANABE	
Development of an Alternative Flame Retardant Gas for Magnesium Melting Furnaces	10
Takaaki FUKATSU	
Design support for outboard motors for small vessels using computational fluid dynamics	15
Masaru SHIMADA Tomoyuki IBA	
Mikio TERADA	
Elucidating the mechanism of hydraulic noise using computational fluid dynamics	18
Masaru SHIMADA	
Method for Designing Lubricant Life	24
Yuma MOCHIZUKI Gou KATOU	
Makoto MAEDA	
Technology to Restore the Performance of used CVT fluids by Adding Additives	28
Akira SUGIMURA Gou KATOU	
Makoto MAEDA	

Design concept and technical verification of low viscosity reducer oil	33
--	----

Kazunori ISHIGAMI	Gou KATOU
Makoto MAEDA	Ryo SASAKI
Hitoshi KOMATSUBARA	

Innovation in the development of CVT unit systems and their applications in projects	38
--	----

Takeshi KANEDA	Toru YOKOTA
----------------	-------------

Introduction to Product

Introducing the Jatco CVT-XS (JF023E) for Nissan KICKS	45
--	----

Introducing the JR913E 9-speed AT for INFINITI QX80, Nissan ARMADA and NISSAN PATROL	46
---	----

Introducing Shift Pulley for BRP-Rotax ATV transmission	47
---	----

Introduction to Patent

POWER TRANSMISSION DEVICE	48
---------------------------------	----



Technology for solving the dilemma between carbon neutrality and economic activity

Hiroyuki KAI
VP

With the extreme heat witnessed this summer and the large-scale disasters caused by frequent extreme weather events worldwide, we are keenly aware that global warming is seriously impacting the entire world. In response to this problem, an international goal for carbon neutrality (CN) has been set, and efforts are being made to limit the rise in global temperatures by reducing greenhouse gas (GHG) emissions. JATCO has also established CO₂ reduction as one of its company-wide KPIs and is promoting activities to address this issue as part of its 18 material sustainability issues.

The main source of CO₂ emissions is the combustion of fossil fuels, especially thermal power generation and automobile engines. Therefore, reducing the dependence on fossil fuels, expanding the use of renewable energy sources, and improving the efficiency of electric energy usage is essential. For example, electric vehicles (EVs) are an effective means of reducing driving emissions and contributing to CO₂ reduction. However, the manufacturing process of EVs, particularly battery production, may emit more CO₂ than conventional gasoline vehicles. Thus, considering CO₂ reduction throughout the entire product lifecycle is necessary.

Energy demand tends to increase with economic activity, leading to higher CO₂ emissions. The dilemma in today's society is that, while emphasis is placed on people's freedom of movement and the pursuit of convenience, as well as on AI-based data processing and learning activities, these activities involve massive power consumption, which increases the burden on the global environment.

In theory, reducing energy consumption and CO₂ emissions is possible by restricting human behaviors and curbing economic activity. However, such an approach contradicts the fundamental elements of economic growth, making it practically unfeasible.

To solve this dilemma, developing renewable energy sources that do not emit CO₂, researching fuels that do not emit CO₂ when burned, and advancing battery technologies with less environmental impact is essential. Improvements in power consumption efficiency have also significantly contributed to CO₂ reduction. For example, the energy management technologies developed in the automotive industry are considered highly effective and will probably play an important role in improving power efficiency.

By holistically promoting these innovations, we believe we can reduce the demand for fossil-fuel electricity and overall CO₂ emissions without compromising economic activity or personal freedom. Our company is committed to contributing to the reduction of CO₂ emissions in these technological fields and is making every effort to realize a sustainable society.

In this issue, we will introduce specific examples of the following two initiatives:

- Development of Energy-Analysis Platform for Carbon Neutrality
- Development of an Alternative Flame Retardant Gas for Magnesium Melting Furnaces

Development of Energy-Analysis Platform for Carbon Neutrality

Taichi KIMURA** Shoji SUZUKI* Masashi KOKAI** Hitoshi WATANABE*

Abstract

To achieve carbon neutrality in the entire value chain by 2050, JATCO is promoting energy conservation through the advancement of DX production and innovation in production technologies. Whereas the visualization of power consumption has been established in each factory area, JATCO has restructured its system to promote power conservation at the operational level in each workplace through a more comprehensive power management.

This paper reports the development of an in-house system that can acquire electricity and air-consumption data in real time for each facility as an energy-analysis platform for achieving carbon neutrality by the production division.

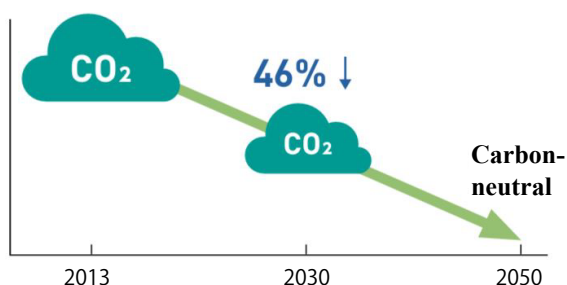
1. JATCO's efforts to reduce greenhouse gas emissions

1.1 Targets in Japan

In April 2021, the Japanese government announced the goal of achieving carbon neutrality by 2050 and a 46% reduction in greenhouse gas emissions by 2030 (compared with FY2013 levels).

1.2 JATCO's goal setting

JATCO aims to achieve carbon neutrality throughout its value chain by 2050 and reduce CO₂ emissions by 46% by 2030 (Fig. 1).



A 46% reduction*
in CO₂ emissions by 2030 *Compared to 2013

Fig. 1 JATCO's Greenhouse Gas Reduction Targets

1.3 Ratio of CO₂ emission in JATCO's production activities

In FY2023, 80% of JATCO's CO₂ emissions from its production activities were from electricity consumption, whereas 20% were from fuel consumption. Therefore, the use of electricity, which emits a significant amount of CO₂, must be reduced (Fig. 2).

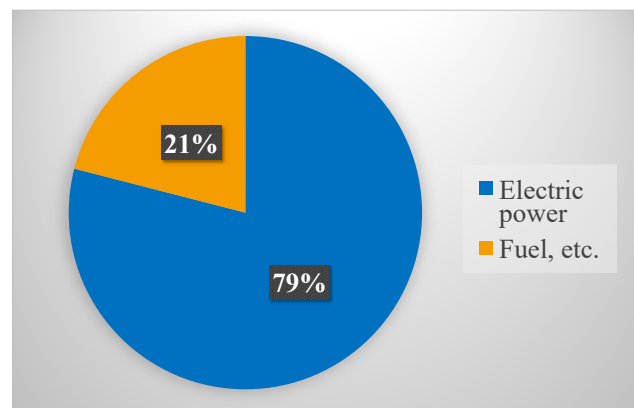


Fig. 2 Percentage of CO₂ emissions from production

1.4 Activities to reduce electricity consumption

The current power-visualization activities are discussed below. Fig. 3 shows a factory floor plan in which power visualization is performed block by block using different colors.

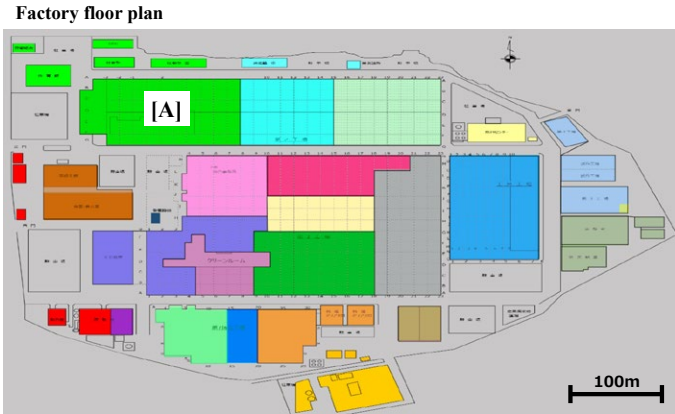


Fig. 3 Schematic diagram of the entire factory

For example, by clicking on the green block [A] in Fig. 3, a graph is displayed, as shown in Fig. 4, which depicts the transition of power consumption in the area within one month. The vertical axis represents the electric energy used (kWh) and the horizontal axis represents the time (h), which can be set arbitrarily.

1.5 Current issues and next steps for power visualization

Power-consumption visualization by factory blocks was performed as described previously. However, a manufacturing site highlighted that power saving did not improve as the electric energy by the equipment in that site was unknown.

To promote energy conservation in factories, one must understand the amount of energy consumed by each piece of equipment as well as identify any waste. Currently, each workplace houses approximately 30 pieces of equipment, although not all are installed with watt-hour meters. The installation of watt-hour meters at each facility requires a significant amount of time and money; thus, it is rarely considered.

Additionally, most equipment in plants use compressed air, and a significant electric power is required to generate compressed air.

Therefore, an in-house system was developed to acquire and understand the power and air-consumption data at each facility.

2. Development Concept

As mentioned above, our company aims to visualize the power consumption at each facility to achieve carbon neutrality.

JATCO's facilities use electricity and air as power sources and employ equipment from various manufacturers. Many commercial products are sold in packages that are inflexible, expensive, and incompatible with other manufacturers' equipment. Therefore, our company has developed an in-house power-visualization and -measurement unit that can be installed universally.

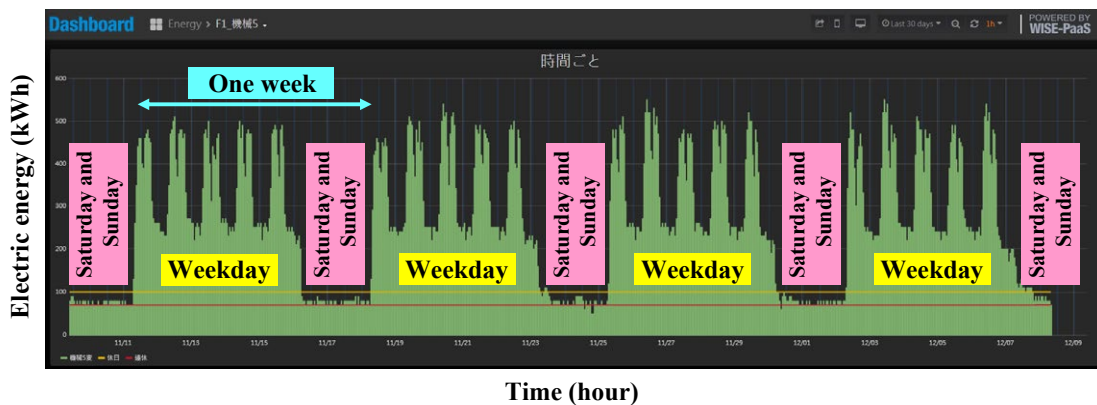


Fig. 4 The power transition of the block

3. Design of power-visualization and -measurement unit

3.1 Configuration overview

The power-visualization and -measurement unit was designed with three components: a Raspberry Pi⁽¹⁾, a power-measurement board, and an uninterruptible power supply (UPS) board.

A diagram of the system configuration, including the power-visualization and -measurement unit, is shown in Fig. 5.

3.2 Selection of Raspberry Pi

JATCO typically uses Raspberry Pi for in-house IoT development. This is because Raspberry Pi is inexpensive, compact, and suitable for driving motors and visualizing equipment status, in addition to being compatible with Python.

3.3 Design of power-measurement infrastructure

Continuous quantitative detection is required to measure the airflow and current consumed by the equipment, and the sensor output is an analog signal. However, because the Raspberry Pi does not have an analog I/F, one must convert its analog signals to digital signals using an analog-to-digital converter (ADC). A power-measurement board was fabricated for this purpose.

3.4 Design of UPS infrastructure

In our assembly facilities, power is turned off during safety inspections of equipment and in emergency situations. Interruption of the power supply may cause equipment failure and data corruption. To address errors that may occur during forced power cutoff, a UPS for Raspberry Pi was created.

3.5 Data flow

The airflow rate was acquired using a flow sensor, and the current consumed by the equipment was obtained using a clamp sensor. The analog current was converted to voltage using a shunt resistor, which was used to detect the current in the circuit. The voltage was converted to a digital signal, whereas the air and electricity consumptions were calculated and sent to the PLC. Data acquisition by the PLC enables connection with the higher system, whereby power visualization becomes possible for each equipment, line, and factory (Fig. 6).

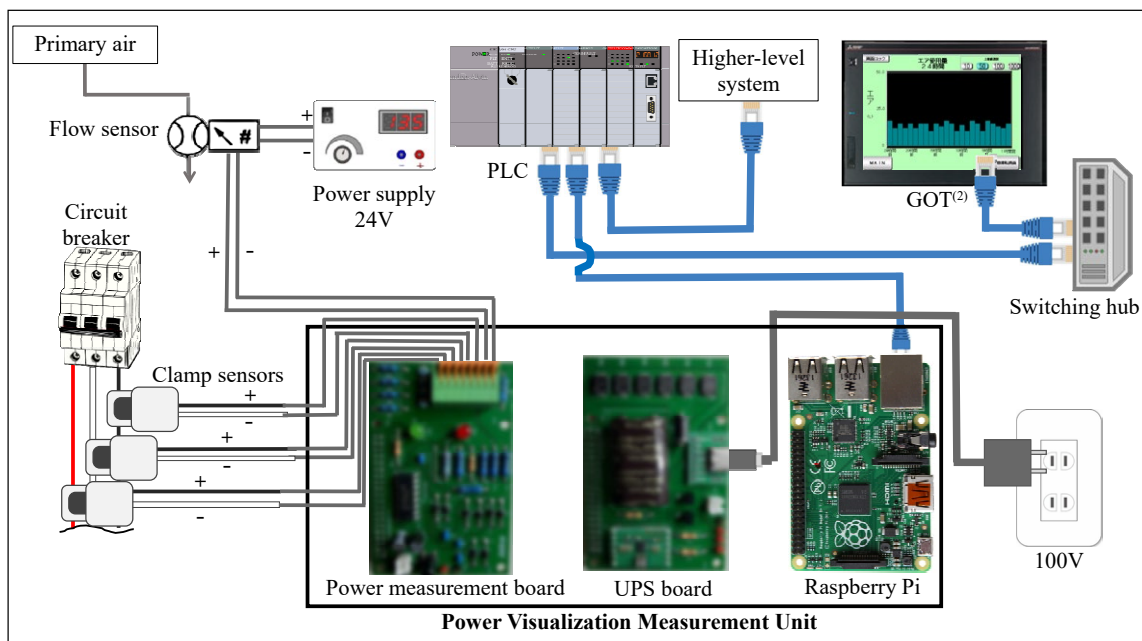


Fig. 5 System configuration

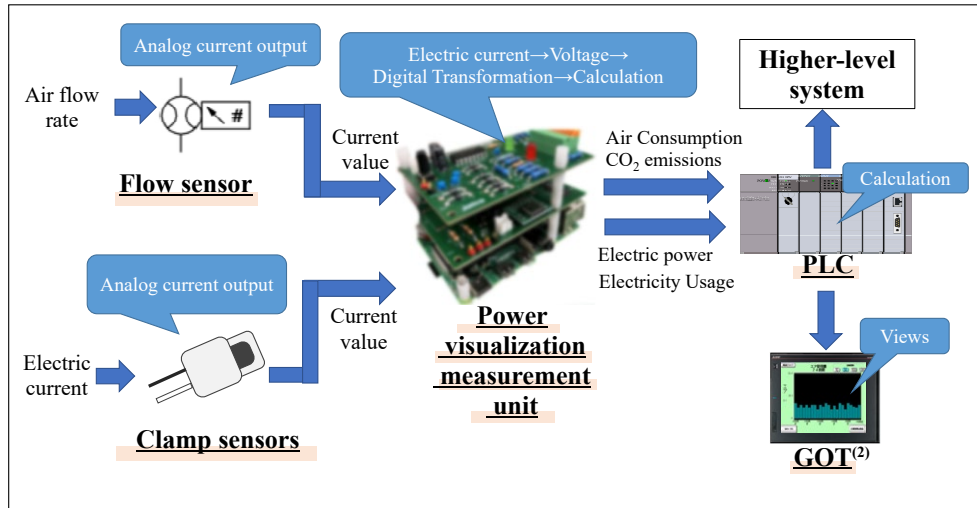


Fig. 6 Data processing flow

4. Development topics

A detailed list of topics that emerged during the development process is provided below.

4.1 Significance of noise suppression

Noise-suppression measures for factory equipment are essential for the safety control, quality control, and stable operation of machines. These measures are important because equipment malfunctions can result in the shutdown of equipment operations, thereby affecting production and safety.

Our factory is located near the Shinkansen bullet train (Fig. 7), where many 200–400 VAC facilities operate in a noisy environment. Hence, robust noise-suppression measures are necessary.

4.2 Examples of noise suppression

Based on knowledge regarding noise-suppression measures for CVT ATCU,

JATCO selected the following six measures to enhance the system reliability.

Measure 1) Detailed implementation of single-point grounding

The circuit and board design ensured single-point grounding.

Measure 2) Optimization of placement of analog and digital signals

To prevent chattering noise in the analog and digital signals on the board, the ADC was placed near the GPIO pin, i.e., the input/output pin of the Raspberry Pi, which is close to the board output. Additionally, the layout was designed to maintain a certain distance between the signals.

Measure 3) Signal-noise reduction

The analog currents were converted to voltage using shunt resistors on the board to improve the noise resistance.

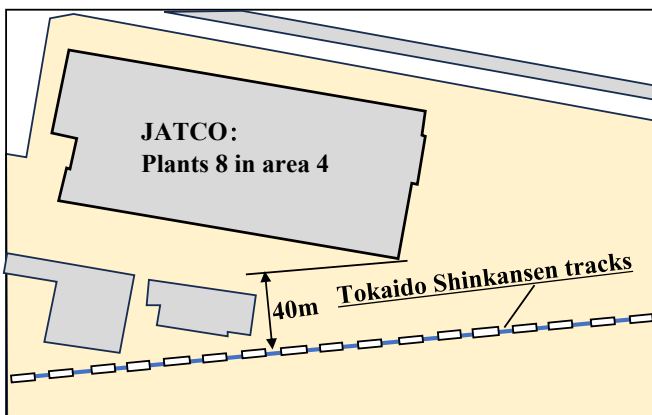


Fig. 7 Distance between Shinkansen and JATCO

Measure 4) Preventative measures for IC malfunction

The IC-free pins were fixed to the GND level via a resistor, and a bypass capacitor was used between the IC power supply and GND to stabilize the power supply.

Measure 5) Measures for signal-input terminals

A low-pass filter was implemented in the input-signal section of the board to eliminate high-frequency noise components. A diode-clamp circuit was constructed to protect the CPU by preventing overvoltage at the input terminal.

Measure 6) Protection using metal casing

The board case was made of a metal with high noise-shielding properties, which protects it from external noise and prevents internal-clock noise generated by the Raspberry Pi from leaking.

4.3 Durability

The durability of the Raspberry Pi used in this study was an issue. Based on previous failures, the following measures were adopted to achieve stable operation over a long duration: A cooling fan was installed to prevent overheating the CPU, a highly reliable power supply unit with a PSE mark⁽³⁾ was selected, and a highly durable and reliable industrial microSD card was used.

5. Verification results

The verification results for the development of the power-visualization and -measurement unit are provided below.

5.1 Verification of noise suppression

As mentioned above, the implementation of noise-suppression measures prevented malfunctions and improved reliability.

5.2 Verification of UPS board

The verification results for the UPS board are shown in (Fig. 8). The horizontal and vertical axes represent time and voltage, respectively. The blue and yellow lines represent the output-signal and UPS power-supply waveforms, respectively. The power supply time of the UPS was 15 s, which was higher than the 10 s required to shut down the Raspberry Pi after the power was cut off, thus verifying that power was maintained.

The details of the graph in Fig. 8 are as follows:

Point A: Start automatic shutdown of Raspberry Pi

Point B: Complete the shutdown of Raspberry Pi

Point C: Turn off UPS power supply

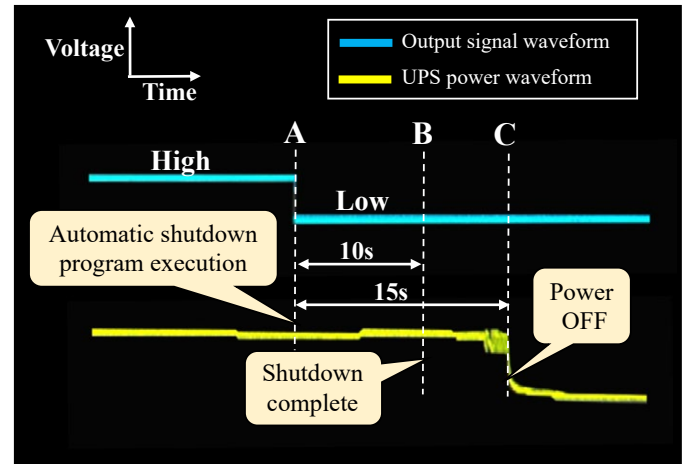


Fig. 8 Verification of the operation of the backup power supply when the power is turned off

5.3 Verification of power-measurement board

As described in the concept-development section, a universal measurement unit was developed. The unit can communicate universally with any commercially available PLC with an Ethernet communication port.

Correlation analysis was performed to verify the accuracy of the measurement unit. For each current value, a comparison was performed between the current measured by the clamp meter (vertical axis) and the current obtained by the clamp sensor attached to the measurement unit (horizontal axis). A strong correlation was observed (Fig. 9). The power value P is expressed as $P = VI$. Because the voltage V is a fixed value, the power value can be determined when the current value is known.

Furthermore, a comparison was performed at each airflow rate between the digital-display value of the flow sensor (vertical axis) and the value calculated using Python from the analog current output measured by the flow sensor (horizontal axis), which showed a strong correlation (Fig. 10). The conversion from airflow rate to power was performed using the conversion coefficient for compressed air at each factory⁽⁴⁾.

The results confirmed that the measurement unit operated accurately.

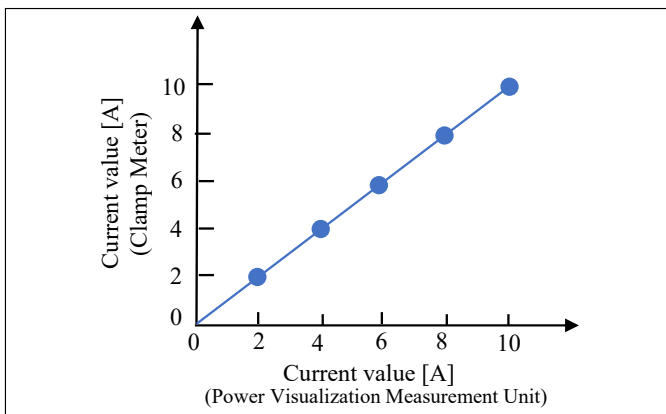


Fig. 9 Relationship between the actual current measured by the clamp meter and the measured current by the measurement unit

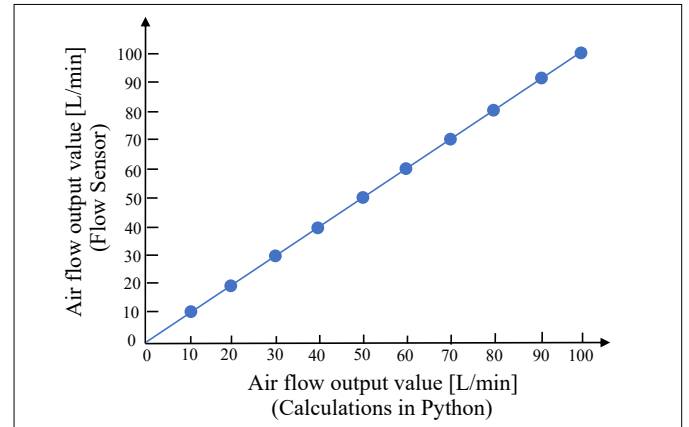


Fig. 10 Relationship between the actual current measured by the air flow sensor and the measured current by the measurement unit

6. Conclusion

An energy-analysis platform was developed to measure the airflow and current consumed by each facility and to visualize the power consumption. This platform was developed to satisfy the requirements of detailed power management and power saving at manufacturing sites. The platform determines the electric energy consumed by each factory facility, thus enabling effective energy conservation activities. The cost of the system was reduced by half, compared with the standard price of commercially available products.

7. Future outlook

Fig. 11 shows a graph that visualizes the total electric-power consumption. The graph was created by installing power-visualization and -measurement units for each piece of equipment. The horizontal axis indicates time, the vertical axis (axis 1) indicates the electric energy, and the vertical axis (axis 2) indicates the number of units produced. The analysis of the measured power consumption revealed that a significant electric power was consumed even during nonproduction hours (standby power) compared with the electric power consumed during production, thus providing ideas for concrete measures to reduce power consumption (CO₂ emission reduction).

The use of a PLC enables various analyses and the utilization of data concomitantly with equipment operation. In the future, extensive test monitoring will be conducted to investigate various reduction measures for achieving carbon neutrality, thus contributing to the goal of reducing greenhouse gas emissions by 46% in FY2028 (compared with FY2013 levels).

- (1) The Raspberry Pi is a trademark registered with the Raspberry Pi Foundation. The photograph of the circuit board cited in this article was obtained from Wikimedia Commons (©2016 Herbfargus CC-BY-SA-4.0).
- (2) GOT is a trademark or registered trademark of Mitsubishi Electric Corporation in Japan and other countries.
- (3) The PSE mark certifies that the electrical appliance satisfies the standards of the Electrical Appliance and Material Safety Law.
- (4) Because compressed air is generated on a plant-by-plant basis using large air compressors, the conversion factor was determined based on the electricity consumption of the compressors.

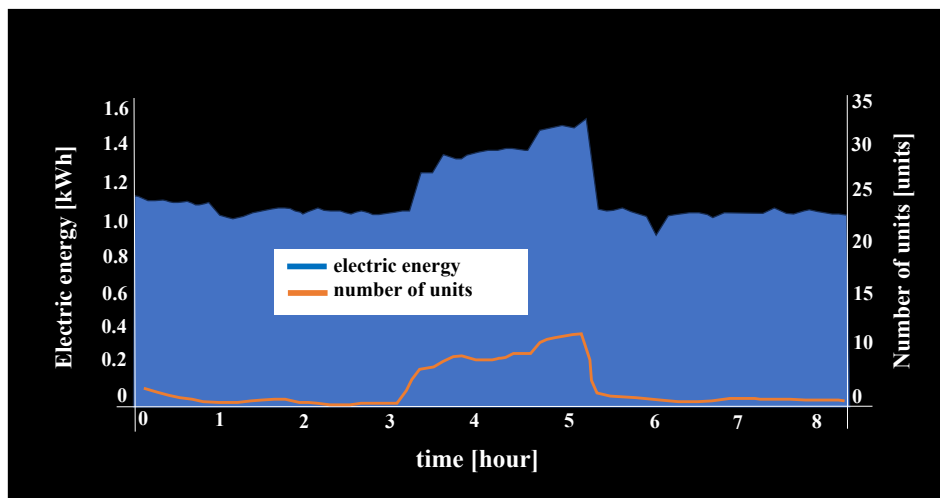


Fig. 11 Total electric energy and number of units produced by the hour

■ Authors ■



Taichi KIMURA



Shoji SUZUKI



Masashi KOKAI



Hitoshi WATANABE

Development of an Alternative Flame Retardant Gas for Magnesium Melting Furnaces

Takaaki FUKATSU*

Abstract

JATCO uses sulfur hexafluoride (SF_6) as a flame-retardant gas in magnesium melting furnaces. SF_6 has an extremely high global warming potential; hence, its replacement with alternative gases is required to meet the carbon-neutral goal. This study reports the evaluation results of preliminary experiments on the adoption of an alternative flame-retardant gas.

1. Introduction

Owing to global environmental issues, it is essential to improve the fuel efficiency of automobiles. Transmissions must not only improve efficiency but also reduce weight. The conventional JATCO transmission case parts were composed of aluminum alloys. The new nine-speed automatic transmission for rear-wheel drive (RWD) vehicles (Fig. 1), for which mass production began in 2019, uses a magnesium (Mg) alloy for the transmission case to achieve a weight reduction of approximately 4 kg.

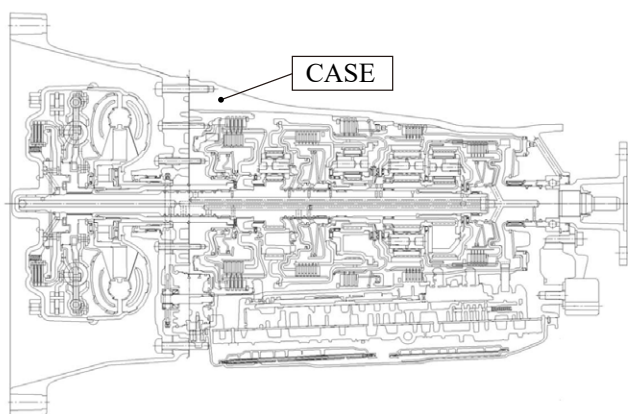


Fig. 1 9-speed automatic transmission for RWD vehicles

A die-casting line dedicated to Mg was constructed in conjunction with the production of a new nine-speed transmission case. The die-casting line consists of a Mg ingot feeder, melting furnace, die-casting machine, and trim press. The flame-retardant gas discussed in this study is used in a Mg melting furnace.

As Mg combusts spontaneously at temperatures $\geq 400^\circ\text{C}$, it is necessary to prevent the combustion of molten metal at temperatures $\geq 600^\circ\text{C}$ using a flame-retardant gas, such as sulfur hexafluoride (SF_6). However, SF_6 has been designated as a target of the Act on Promotion of Global Warming Countermeasures. SF_6 has a global warming potential (GWP) approximately 23,000 times that of CO_2 . The Mg casting line of JATCO is one of the largest in Japan in terms of production weight, and SF_6 comprises 8% of the greenhouse gases emitted by JATCO (Fig. 2). Therefore, it is necessary to develop an alternative gas to SF_6 to achieve a 46% reduction (compared to FY2013) in greenhouse gas emissions by FY2028.

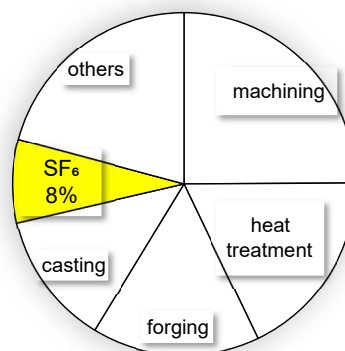


Fig. 2 Ratio of CO_2 emission

*Casting & Forging Plant

2. Selection of alternative gases

Five potential alternative gases were selected as replacements for SF_6 , as shown in Table 1⁽¹⁾. Three factors were evaluated for gas selection: GWP, half-lethal concentration (LC50), and perfluorinated organic compounds (PFAS) regulation.

First, regarding gas (1) SO_2 , even the presence of trace amounts in the air is a concern for human health as even a low LC50 value poses a high risk. Strict environmental standards for gas (1) have been established in Japan, restricting its adoption. However, gases (2)-(4) are expected to fall under PFAS regulations, and their use and production are expected to be banned in the future. As there were cases in which the production of gas was suspended owing to PFAS regulations, the adoption of gases (2)-(4) was discarded. Therefore, gas (5) trifluoroiodomethane (CF_3I) was selected as a substitute for SF_6 . The GWP of CF_3I was 0.4 times that of CO_2 , which is a significant improvement over the GWP of SF_6 , which was 23,000 times that of CO_2 . CF_3I has not been used as a flame-retardant gas for Mg; hence, preliminary experiments were necessary.

Table 1 Alternative gases

Alternative gases	GWP	LC50 (ppm)	PFAS Regulation Applicable	Practical Use for magnesium
(1) SO_2	0	2,520	No	Yes
(2) $\text{C}_3\text{F}_6\text{O}$	1	>100,000	Yes	Yes
(3) HFC134	1,300	350,000	Yes	Yes
(4) OHFC-1234ze	30	>100,000	Yes	Yes
(5) CF_3I	0.4	>100,000	No	No

3. Experimental procedure

3.1 Evaluation method

The performance of flame-retardant gases must be evaluated based not only on their flame-retardant characteristics, but also on the potential generation of toxic gases due to chemical reactions in the furnace and their effect on casting quality. This study focuses on flame-retardant properties. Flame-retardant properties are often evaluated based on the binary value of whether a material burns. In this study, a quantitative evaluation method was investigated. As the combustion of Mg is the reaction $2\text{Mg} + \text{O}_2 \rightarrow 2\text{MgO}$, it was considered that the degree of combustion (flame-retardance) could be evaluated using the amount of magnesium oxide (MgO) generated. Therefore, the molten metal surface was divided into 20 sections, as shown in Fig. 3, and the presence of MgO was determined for each section. The percentage of MgO on the molten metal surface was considered as the MgO generation rate.



Fig. 3 Inflammability evaluation

3.2 Experimental conditions

Preliminary experiments were conducted in a 50 kg melting furnace owned by the Ibaraki Prefecture Industrial Technology Innovation Center (Fig. 4).



Fig. 4 Melting furnace for experiment

The flame-retardant gas was supplied to the molten surface using a carrier gas, such as N_2 or CO_2 . When molten Mg reacted with CF_3I , magnesium fluoride (MgF_2) was formed on the molten metal surface (Fig. 5). The formation of the MgF_2 film impeded contact between oxygen and the molten metal, preventing combustion. The flame-retardant gas was thermally decomposed upon exposure to high temperatures in the furnace, and its performance degraded.

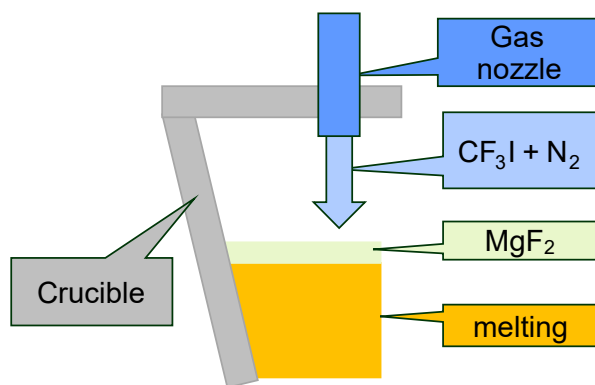


Fig. 5 Flame retardant film MgF_2

Therefore, it was considered that the amount (concentration) of the flame-retardant gas, carrier gas, and temperature of the molten metal affect the formation of flame-retardant films.^{(2),(3)} Three levels of investigation were conducted for each factor to determine their degree of influence.

After setting the prescribed experimental conditions, such as the gas and molten metal temperatures, MgO was removed from the surface of the molten metal, and the molten metal was allowed to stand for 2 min. The rate of MgO generation on the surface was observed to evaluate the flame-retardant characteristics.

The experimental conditions for alternative gases were as follows:

- (i) Melting furnace: 50 kg melting furnace.
- (ii) Mg alloy material: AS31.
- (iii) Flame-retardant gas: CF_3I .
- (iv) Concentrations of flame-retardant gas: 250, 500, and 1,000 ppm
- (v) Carrier gases: N_2 , $N_2 + CO_2$ mixture, and CO_2 .
- (vi) Molten-metal temperature: Base - $20^\circ C$, base (temperature of the actual equipment), and base + $20^\circ C$.
- (vii) Furnace lid: Open.
- (viii) Duration of experiment: 2 min.

4. Results

Experiments conducted using actual equipment under actual production conditions (SF_6) resulted in an MgO generation rate of 40%. This value was set as the target value for CF_3I .

The results of the tests on CF_3I are described below. First, the flame-retardant characteristics of the flame-retardant gas were evaluated at each concentration. Fig. 6 shows the results of the experiments conducted under conditions where the molten-metal temperature was the same as that of the actual equipment (base), the carrier gas was fixed as N_2 , and the CF_3I concentrations were 250, 500, and 1,000 ppm. It was found that the higher the CF_3I concentration, the higher the flame-retardance, and that a CF_3I concentration of 500 ppm resulted in flame-retardance that was almost equivalent to that of SF_6 .

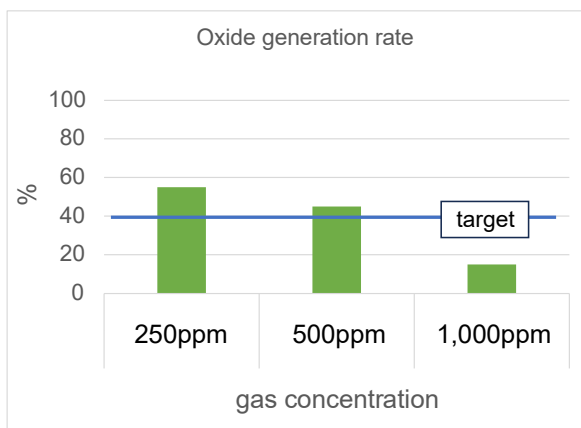


Fig. 6 Inflammability evaluation of gas concentration

Subsequently, the flame-retardant characteristics of each carrier gas were evaluated. Fig. 7 shows the results of the experiments conducted under the conditions of a 500 ppm CF_3I concentration, the same molten-metal temperature as that of the actual equipment (base), and three carrier gas types (N_2 only, a mixture of N_2 and CO_2 , and CO_2 only). It was revealed that the CO_2 -only condition resulted in a higher flame-retardance. However, under CO_2 -only conditions, the toxic gas hydrogen fluoride (HF) was generated, which corroded the metals in the furnace. Therefore, a mixture of N_2 and CO_2 gases was used for further investigation.

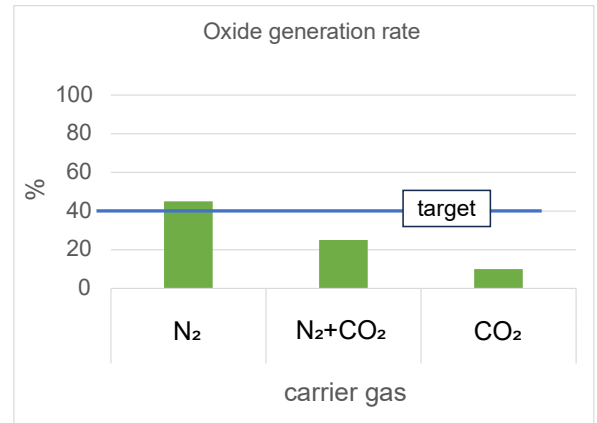


Fig. 7 Inflammability evaluation of carrier gases

Next, the flame-retardance was evaluated at different molten metal temperatures. Fig. 8 shows the results of the experiments conducted under the conditions of a flame-retardant gas concentration of 500 ppm, carrier gas of an $\text{N}_2 + \text{CO}_2$ mixture, and molten metal temperatures of base - 20 °C, base, and base + 20 °C. The flame-retardant properties decreased at higher molten metal temperatures and increased at lower molten metal temperatures.

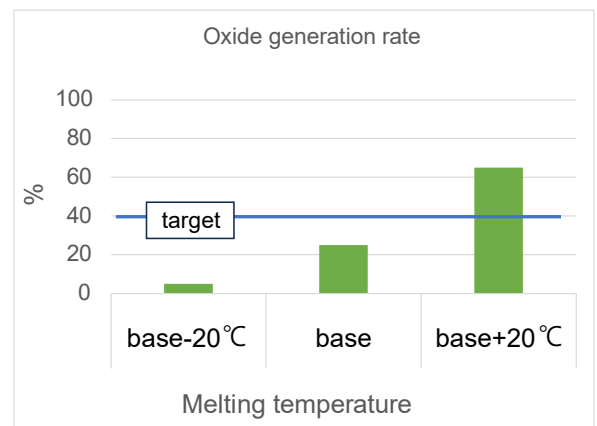


Fig. 8 Inflammability evaluation of melting temperature

5. Discussion

The experimental results are discussed below.

As for the effect of the CF_3I concentration, the flame-retardance improved with higher concentrations. This was because a sufficient amount of CF_3I was supplied to the molten metal surface, facilitating the formation of a flame-retardant film.

Regarding the effect of the carrier gas, flame-retardance improved with higher amounts of CO_2 . This was because the specific gravity of CO_2 is higher than that of N_2 , and CF_3I readily reached the molten metal surface before CF_3I thermally decomposed, which facilitated the formation of a flame-retardant film. However, when a CO_2 -only carrier gas was used, HF was generated, and corrosion was observed on the metal parts in the furnace. Therefore, the amount of mixed CO_2 must be maintained at a level that does not generate HF. It was confirmed that when a mixture of N_2 and CO_2 gases was used at a specified ratio, the generated HF was lower than the environmental standard value.

With respect to the effect of the molten metal temperature, the flame-retardant properties decreased at higher molten metal temperatures. This was because CF_3I was pyrolyzed before reaching the molten metal surface, resulting in insufficient formation of the flame-retardant film. Although it is possible to increase the temperature of the molten metal to improve the casting quality, it is necessary to take measures such as preventing the molten metal temperature from being set above a predetermined temperature to prevent combustion.

6. Summary

The experimental results in this study enable the determination of the conditions under which flame-retardant properties higher than those of SF_6 can be obtained. Hence, CF_3I was judged to be applicable in actual production facilities. The use of CF_3I is expected to reduce the greenhouse gases emitted by JATCO by 8%, thereby mitigating global warming. The use of CF_3I as a flame-retardant gas for Mg melting furnaces is the first such attempt in Japan, achieving compliance with PFAS regulations.

7. References

- (1) TAIYO NIPPON SANSO K.K.: New cover gas for magnesium alloy molten metal, MG Shield, TAIYO NIPPON SANSO Technical Report No. 23 (2004), P1.
- (2) TOSEI K.K.: Research on the applicability of magnesium alloy manufacturing process, Development of Energy-saving Synthetic Technologies for Fluorocarbon Replacements, (May 2007), P2-P7.
- (3) Ahresty K.K.: Applicability study of magnesium alloy manufacturing process, Development of Energy-saving Synthetic Technologies for Fluorocarbon Replacements (March 2007).

■ Authors ■



Takaaki FUKATSU

Design support for outboard motors for small vessels using computational fluid dynamics

Masaru SHIMADA* Tomoyuki IBA* Mikio TERADA*

Abstract

Part-design support was provided to the Marine Division of Yamaha Motor Co., Ltd. using computational fluid dynamics (CFD) technology that our company built through the development of automatic transmissions. Our knowledge of fluid dynamics, technologies of simulation, and data processing was fully utilized through the selection of CFD software, data processing ingenuity and a detailed analysis of the flow field. Consequently, we were able to satisfy the needs of our customers, and we received excellent customer feedback.

1. Introduction

Various studies have been conducted on heat and fluid dynamics to develop automatic transmissions for automobiles. The thermal and fluid phenomena inside transmissions are complex and diverse. For example, in a hydraulic system, there exist multiscale problems in which phenomena ranging from several micrometers to several hundred millimeters must be solved simultaneously. Additionally, problems exist regarding hydraulic response delays and pressure wave propagation when air is mixed with oil. Lubrication systems suffer from problems such as oil agitation by gears, forced lubrication, and cooling of high-speed rotating clutches, pulleys, and bearings. Hence, a wide range of advanced simulation and analysis techniques is required to understand and visualize these phenomena.

This report describes our recent application of fluid analysis technology to support the design of parts for the Marine Division of Yamaha Motor Co., Ltd.

2. Overview of Design Support

2.1 Overview of Simulation

The object of the simulation is the gearbox (red frame) of an outboard motor for small vessels, as shown in Fig. 1.

The oil behavior was analyzed in detail to reduce churning loss. Considering the purpose of the analysis and possibility of the future refinement of the study design, air needed to be considered to computationally reproduce this phenomenon. Hence, the simulation was conducted using SIMULIA XFlow (hereafter referred to as XFlow)⁽¹⁾, which is a general-purpose thermal fluid dynamics simulation software that can accurately calculate gas-liquid two-phase flows.

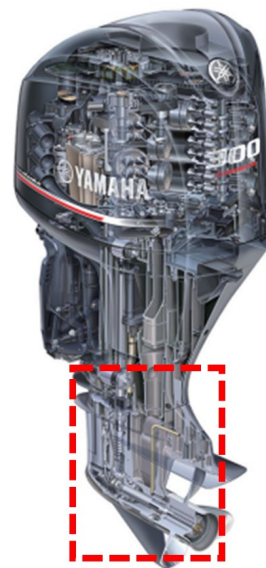
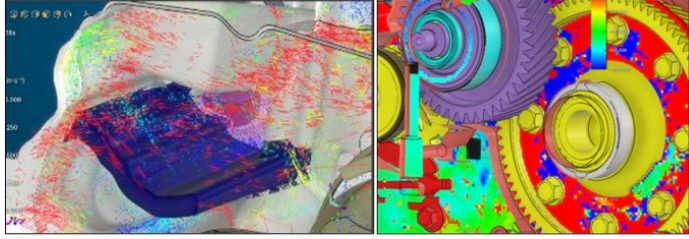


Fig. 1 Outboards for Small Vessels

*Hardware System Development Department, JATCO Engineering Ltd

XFlow has good analytical accuracy, but it also has drawbacks in detailed post-processing, including display problems, such as the velocity vectors being too small to see and the pressure distribution being drawn roughly (Fig. 2).



(a) Velocity vector (b) Pressure distribution

Fig. 2 XFlow results display example

In the development of automatic transmissions, these drawbacks did not present any issues, as the main outputs were the macroscopic behavior of the oil and churning loss caused by the gears. However, for current purposes, these drawbacks pose a major issue. We attempted to solve this problem by loading the XFlow output into STAR-CCM+⁽²⁾, which is another CFD software that has excellent visualization and data processing functions.

2.2 Overview of Analysis

When analyzing the flow in a gearbox, the turbulence components must be handled carefully. When the flow is stirred by the gears, the flow changes constantly owing to interface fluctuations and vortices of various sizes. Therefore, the same procedure cannot be repeated. Moreover, an accurate analysis cannot be performed if only the flow field is used at a particular moment; such an analysis may lead to erroneous judgments. In this study, the turbulence components were removed by averaging the data. As simple time averaging cannot correctly preserve the data on the gear surface, we focused on the gear phase and performed ensemble averaging by extracting and averaging only the data obtained when the gear teeth were in exactly the same position (Fig. 3).

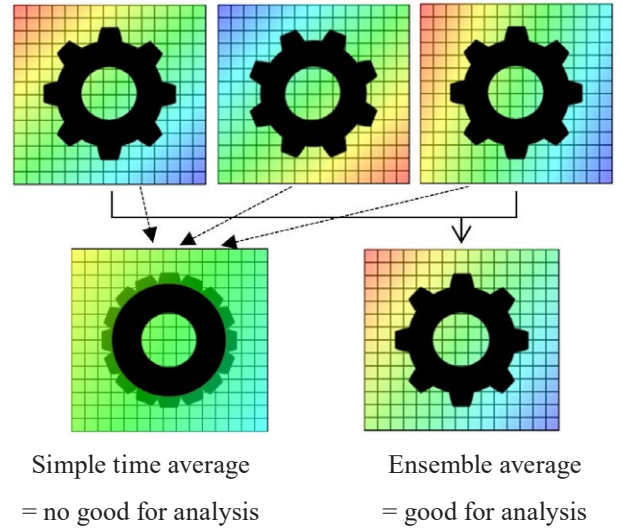


Fig. 3 Data processing method

This allowed only the time-averaged components corresponding to the phase of the gears to remain, thereby ensuring that the phenomena of interest were captured.

However, the following issues must be overcome when transferring the XFlow results to STAR-CCM+.

- 1) The data output from XFlow was not in a format that could be read using STAR-CCM+.
- 2) Even if the phases of the gears are the same, the phases of the bearings, shafts, and so on may not be aligned. These differences result in variations in the sequence of the output data in the result file at each time point, which impedes ensemble averaging. That is, the lines written in each file are different, even though the data are taken from the same location.

These issues were addressed using data processing programs. For Issue 1), the data format was rewritten using AWK, which is a language that specializes in processing text data. Next, Issue 2) was addressed using the data-mapping function in STAR-CCM+. First, a unified mesh was prepared, in which rotators with different phases were removed from the model. The resulting files written at each time point were read, mapped, and output sequentially. As there were 200 result files, Java programming was used to automate the entire process to accelerate and improve the work efficiency.

Consequently, data from the same location are always written on the same line, which makes data processing easier. In

addition, a simple program was written using AWK to perform ensemble averaging.

Figure 4 shows an example of the flow analysis. Using data with minor turbulence components, it was possible to perform a detailed analysis and evaluation of the pressure distribution, velocity distribution, and their relationship with the torque loss. This analysis enabled the identification of the design parameters that were closely related to the loss of torque, which led to the clarification of the design guidelines.

3. Overview of Design Support

For the first time, fluid dynamics technology has been used to provide design support for components outside the automotive industry. Although this study involved a component with which we had no previous experience, we were able to satisfy the needs of our customers by fully utilizing our knowledge of fluid dynamics, analytical technology, and data processing

technology with programming, which we acquired through the development of automatic transmissions. Consequently, we achieved a high level of customer satisfaction. We will continue to refine our technology and make technical contributions to a wide range of customers.

(1) SIMULIA is a European company (Societas Europaea) incorporated under the laws of France, and is a trademark or registered trademark of Dassault Systèmes that is registered with the Commercial Court of Versailles under registration number 322 306 440, or a trademark or registered trademark of any of the subsidiaries of Dassault Systèmes in the United States or other countries.

(2) STAR-CCM+ is a registered trademark of Siemens AG.

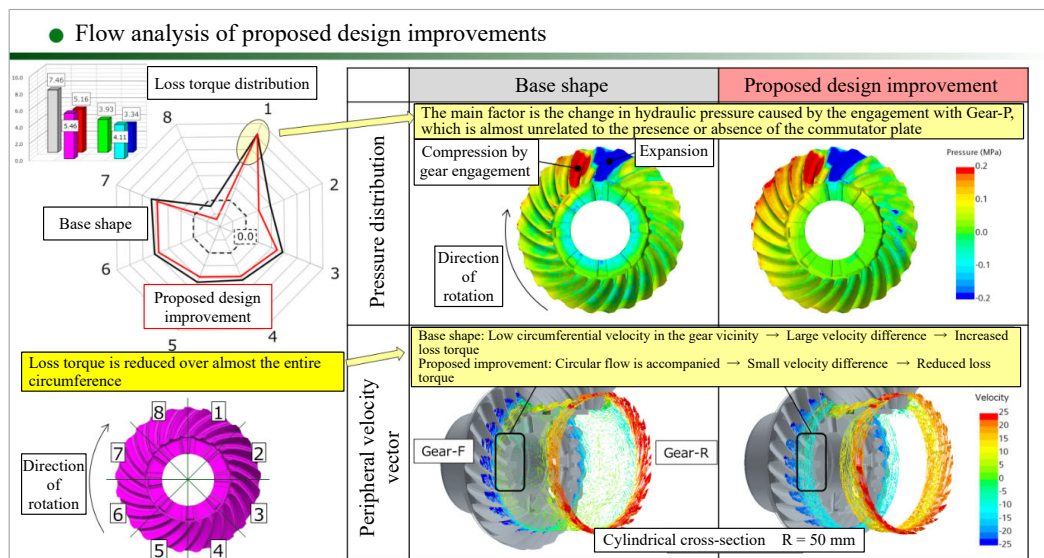


Fig. 4 Example of data analysis

■ Authors ■



Masaru SHIMADA



Tomoyuki IBA



Mikio TERADA

dating the mechanism of hydraulic noise
using computational fluid dynamics

Masaru SHIMADA*

Abstract

Hydraulic system noise has often been addressed experimentally through trial and error. In this study, computational fluid dynamics (CFD) was applied to analyze hydraulic noise, enabling the reproduction of valve regulating pressure behavior and detailed examination of the flow field. The results revealed a mechanism where air entrained in the oil expands and compresses within the circuit, generating noise—a phenomenon that is challenging to investigate through experimental methods alone. This paper details the mechanisms underlying the noise and proposes effective countermeasures.

1. Introduction

NVH (Noise, Vibration, and Harshness) is a critical consideration in transmission development. In particular, hydraulic system noise poses significant challenges due to the complexity of the system and the large number of components involved, making pinpointing the noise source and understanding its underlying mechanism difficult. Consequently, trial-and-error experiments are often employed, such as alternating operating conditions to identify noise-inducing factors or recombining components to determine their contribution to the noise.

In recent years, however, the adoption of computational fluid dynamics (CFD) has become essential in hydraulic system design. CFD enables precise and quantitative evaluations, facilitating decision-making in addressing hydraulic issues.

This paper presents a case study in which CFD was applied to analyze noise in hydraulic transmission systems with the following objectives: (1) to identify the noise source, (2) to estimate the underlying mechanism, and (3) to verify the proposed mechanism. The focus was on noise generated immediately after shifting from N to D range while the engine was running.

2. Narrowing down the issues through experiments

2.1 Narrowing down the noise source

Figure 1 shows a schematic diagram of the hydraulic system of an automatic transmission (hereinafter referred to as “AT”). In an AT, the oil in the oil pan is pumped to various components using an oil pump, where the control valves regulate the pressure and flow of the distributed oil. A pressure regulator valve is located upstream of the control valve. In the system in which noise is generated, a lubrication regulator valve is located immediately downstream of the pressure regulator valve, and the hydraulic pressure in the lubrication circuit is controlled.

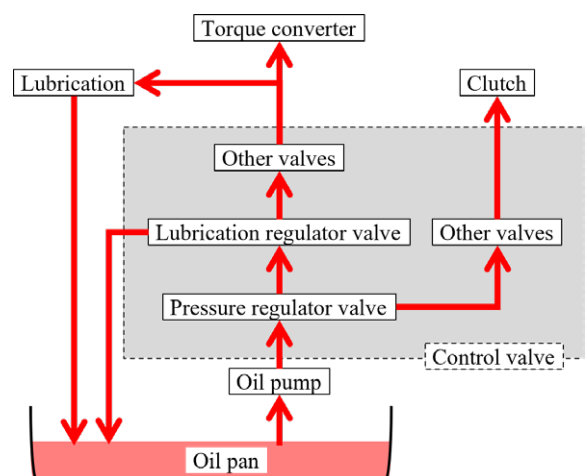


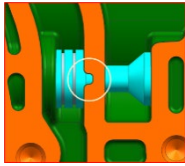
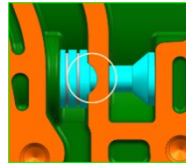
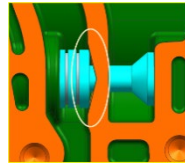
Fig. 1 Schematic diagram of hydraulic system

*Hardware System Development Department, JATCO Engineering Ltd

Initially, noise-generation sites were roughly identified through experimentation. Given the timing of the noise occurrence, only the pressure regulator valve and the lubrication regulator valve were active during the shift operation. This allowed the noise source to be narrowed down to one of these two valves. However, as shown in Fig. 2(a), the proximity of the two valves makes conclusively determining the noise source impossible using experimental noise observation alone.

regulator valve. Consequently, definitively identifying the noise source was still not possible.

Table 1 Noise reduction by notch shape

Original shape	Cylindrical notch	Triangular notch
		
Noise occurred	Noise reduced	Noise reduced

2.2 Narrowing down the causes of hydraulic noise

From experience, three possible factors cause hydraulic noise.

Factor 1: Vibration of components due to the oscillation of hydraulic pressure

Factor 2: Vibration of components due to pressure fluctuations during vortex release

Factor 3: Pressure fluctuations due to air expansion/compression

First, to evaluate Factor 1, the line pressure was experimentally measured during the noise generation using the original notch shape (Fig. 3). The results showed that the hydraulic pressure did not oscillate during, before, or after the noise generation. This finding ruled out Factor 1 as a potential cause of the noise. However, Factors 2 and 3 could not be investigated through this experiment alone, necessitating further refinement and analysis.

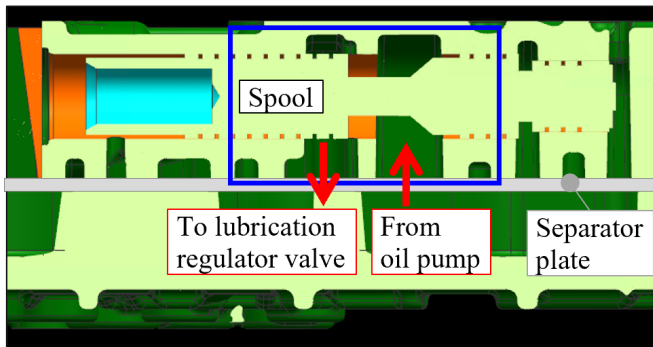
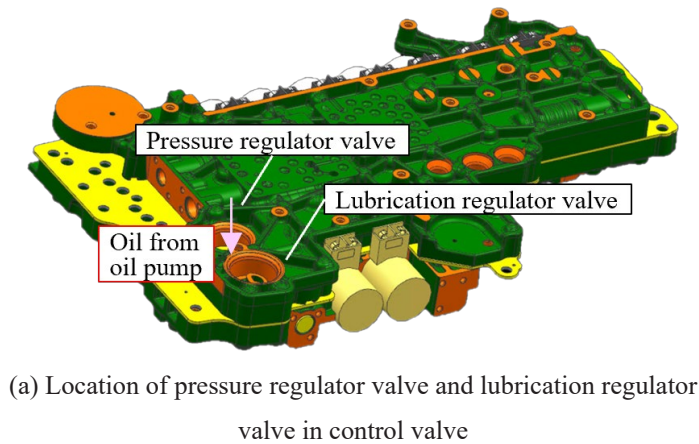


Fig. 2 Control valve and pressure regulator valve

To address this, the notch shape of the pressure regulator valve is modified, as detailed in Table 1, and the resulting noise levels are observed. The notch shapes, viewed from below in the blue frame of Fig. 2(b), include cylindrical and triangular designs. The results revealed that both alternative shapes reduced the noise level compared to the original design. However, the possibility remained that altering the shape of the pressure regulator valve could influence the behavior of the lubrication

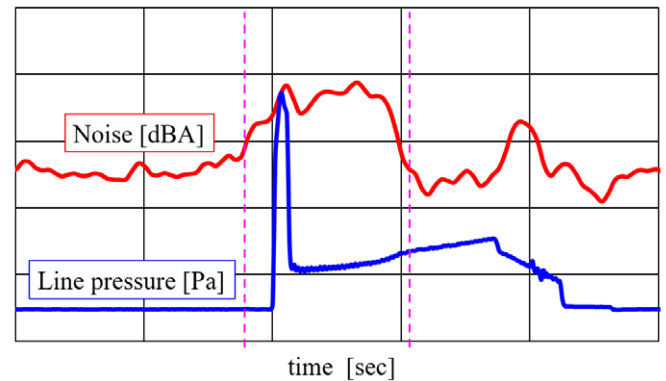


Fig. 3 Noise and line pressure over time

3. Elucidating hydraulic noise mechanism using computational fluid dynamics

3.1 Noise source identification

CFD was applied to address the experimental limitations in identifying the sources and causes of the noise. First, to narrow down the focal area, a noise-generating valve was identified.

As shown in Table 1, the noise volume changes with modifications to the notch shape. This suggests that either the pressure regulator valve, the lubrication regulator valve, or both had altered their regulating states. To confirm the pressure-regulating states for the three notch configurations, simulations were conducted using STAR-CCM+, a general-purpose thermal-fluid dynamics solver. The hydraulic circuits associated with both the pressure regulator and lubrication regulator valves were analyzed. The motion of each spool was solved using the fourth-order Runge-Kutta method, while a sliding mesh and morphing (mesh movement and expansion/contraction) were employed to reproduce the spool motion accurately.

Figure 4 illustrates the time variations in output pressure and spool position for the pressure regulator and lubrication regulator valves. The analysis revealed no significant changes in the output pressure or spool position for the lubrication regulator valve with the notch modifications. In contrast, the pressure regulator valve exhibited substantial changes in both output pressure and spool position. These results confirm that the pressure regulator valve, rather than the lubrication regulator valve, is the noise source.

3.2 Estimation of mechanisms

3.2.1 Cause analysis: Vortex release

When an orifice or another aperture is present in the circuit, periodic vortices may form downstream of the orifice, and the pressure fluctuations caused by the vortex release may induce vibrations in the components, resulting in noise generation (Factor 2). Figure 5 shows a typical example of flow analysis through an orifice, where the colors represent the pressure distribution. The oil flowed from top to bottom, with positive and negative pressures aligned downstream of the orifice, indicating that vortices were periodically released at this location. The separator plate could vibrate due to these pressure fluctuations, generating noise.

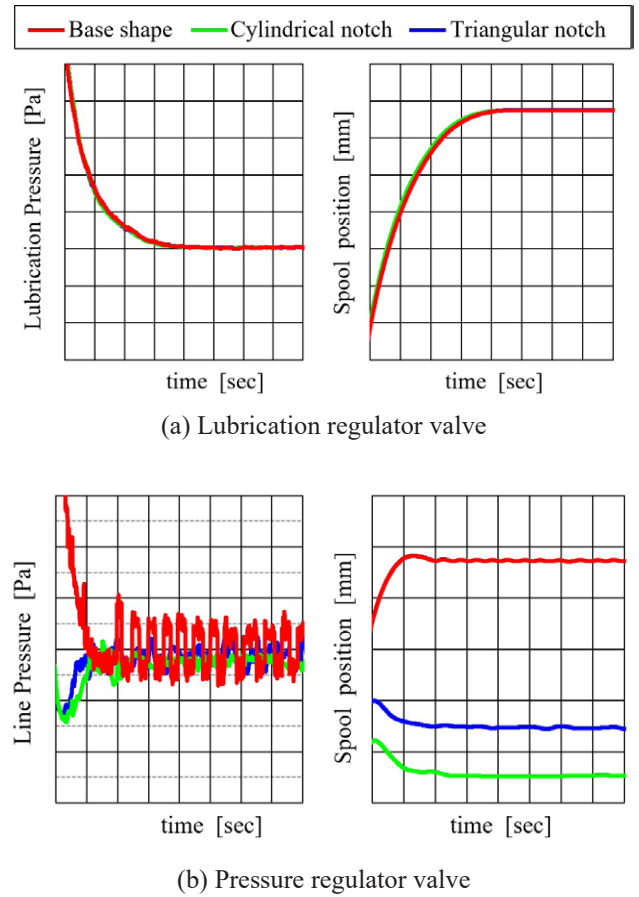


Fig. 4 Pressure and spool position over time

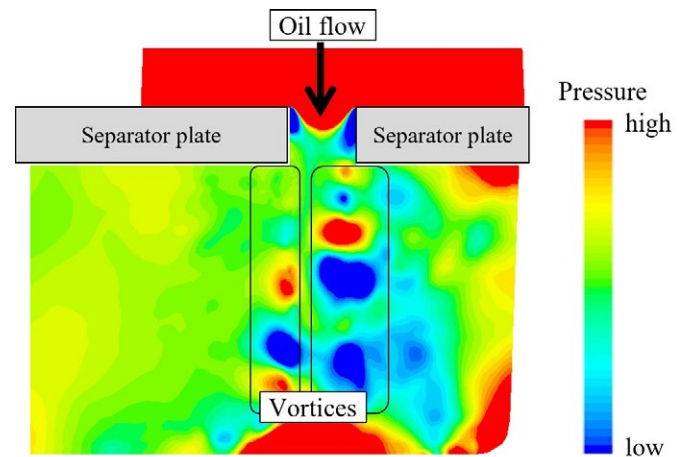


Fig. 5 Pressure distribution in orifice flow

In Figure 6, it can be observed whether a similar phenomenon occurs in the pressure-regulator valve. This shows the pressure distribution during pressure regulation. No periodic release of vortices is evident near the separator plate (in the solid-line enclosure), which has the potential to vibrate. This indicates that the noise is not caused by vortex emission.

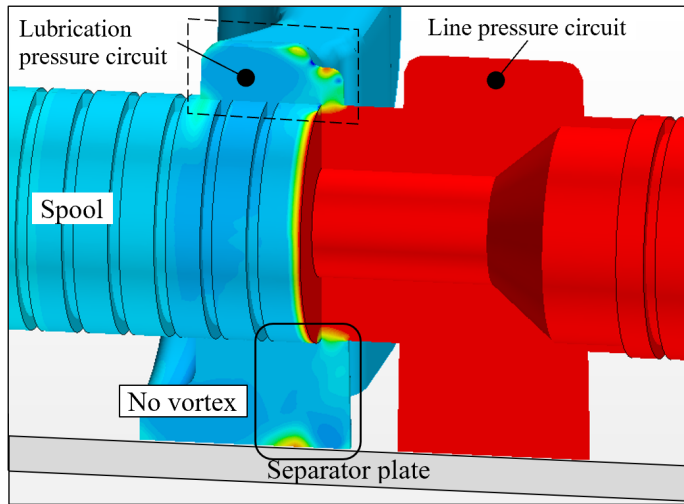


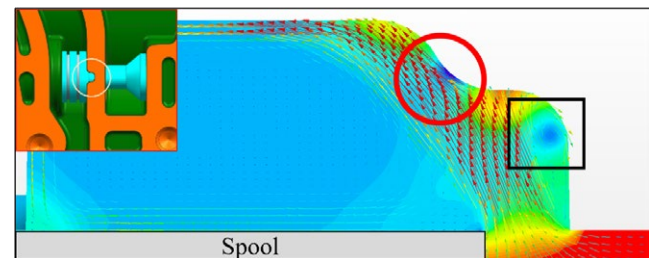
Fig.6 Pressure distribution around pressure regulator valve

3.2.2 Cause analysis: Air expansion/compression

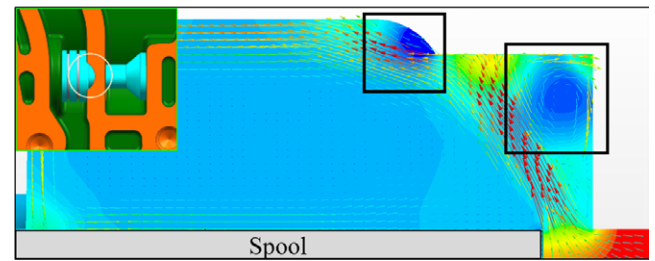
Another possible cause is pressure fluctuations due to air expansion and compression. The oil circulating in the transmission contains fine air bubbles, only a few percent by volume at atmospheric pressure. Strange noises reported in the past were caused by air expansion when drained from the hydraulic circuit to the oil pan, i.e., at atmospheric pressure. However, hydraulic pressure was applied to all connected circuits at the pressure regulator valve, identified as the noise source in this study. Therefore, the critical question is whether air expansion and compression are sufficient to generate noise in such a pressurized state.

The pressure distribution on the opposite side of the separator plate (inside the dashed-line enclosure in Fig. 6) was investigated for the original, cylindrical, and triangular notch shapes, all of which exhibited different noise volumes (Fig. 7).

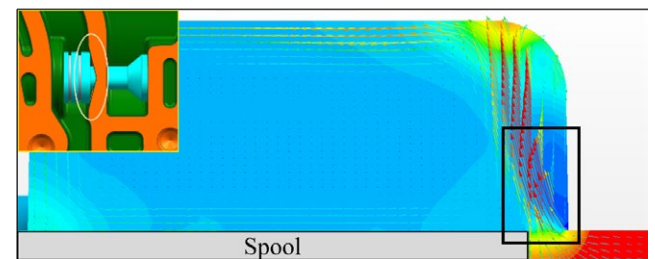
For all notch shapes, a strong low-pressure region, responsible for air expansion, is identified. Simultaneously, two types of air inflators became evident. The first, enclosed by black rectangles, is formed by a vortex created due to flow separation, where pressure decreases at the vortex center. In such cases, the vortex fluctuation significantly affects the noise volume. However, in the present configuration, the position of the separation is fixed at the notch opening or step edge, and the position of vortex formation does not change significantly with the notch shape.



(a) Original shape



(b) Cylindrical notch



(c) Triangular notch

Fig.7 Pressure distribution and velocity vector at lubrication pressure port of pressure regulator valve

Therefore, even if the air expands because of the low pressure, the pressure fluctuation is considered relatively small, and the noise volume is considered low.

In contrast, in the area circled in red, the flow path narrows due to the step, causing an increase in flow speed and resulting in a low-pressure region. This mechanism is similar to cavitation in a hydrofoil⁽¹⁾, where bubbles in a jet stream expand rapidly in the low-pressure zone and compress rapidly after passing through it. This rapid compression of bubbles probably produces significant pressure fluctuations akin to cavitation, generating noise. The low-pressure zone associated with this mechanism is present only for the original notch shape and is absent in the other two shapes, where noise is reduced. This suggests that the primary cause of the noise is the rapid expansion and compression of air due to the localized increase in flow speed and the corresponding decrease in pressure caused by flow condensation.

4. Verification of mechanism

The estimated noise mechanism was next verified by experiments and computational fluid dynamics. Because noise is thought to be caused by the expansion of air in the oil due to a pressure drop, an increase in the lubrication pressure, which is the surrounding pressure, is expected to suppress the pressure drop in the low-pressure region and, in turn, reduce the noise.

Figure 8 shows the CFD results when the lubrication pressure increased for the original notch shape. Compared with Fig. 7(a), the decrease in the step pressure indicated by the red circle is suppressed by increasing the lubrication pressure.

Figure 9 shows the calculated results for the relationship between the lubrication pressure and step pressure. Evidently, a near-linear correlation exists between the lubrication pressure and step pressure.

In addition, the magnitude of the noise was measured with increasing lubrication pressure (Fig. 10). Clearly, the noise decreased as the lubrication pressure increased. This result presents the following clear correlation: “noise decreases as step pressure increases,” and validates the assumed mechanism. Simultaneously, the noise problem was solved by increasing the lubrication pressure during the N-D shift.

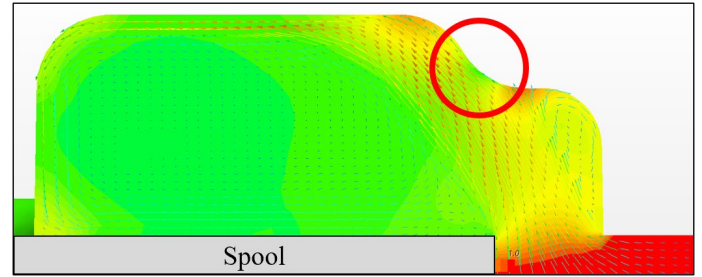


Fig. 8 Pressure distribution and velocity vector at lubrication pressure port of pressure regulator valve
- lubrication pressure is higher than original

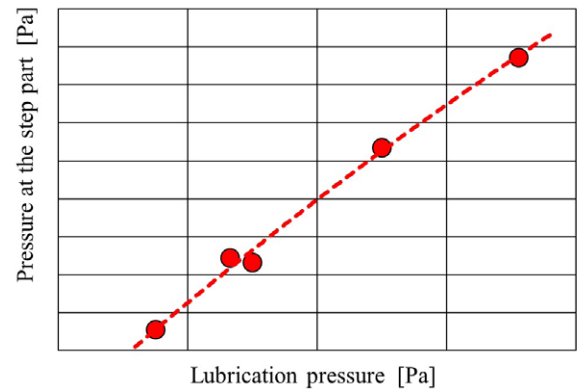


Fig. 9 Relationship between lubrication pressure and step part pressure

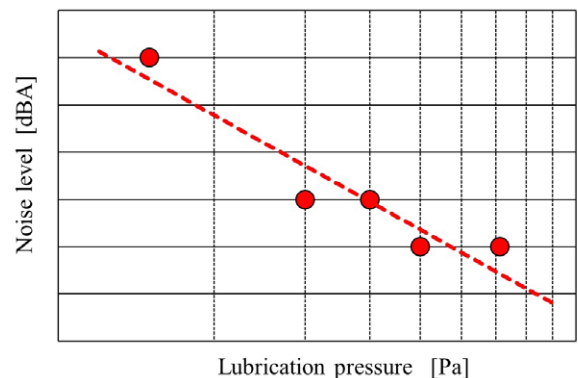


Fig. 10 Relationship between lubrication pressure and noise level

5. Summary

The following results were obtained by applying CFD to hydraulic system noise, which previously required considerable time and cost to solve through trial-and-error experiments:

- ① The sound source can be easily identified by applying a regulating pressure analysis that enables quantitative evaluation.
- ② By visualizing phenomena that could not be observed in experiments, the mechanism of noise generation could be estimated simply by examining the CFD results, even if the mechanism had never been experienced before.
- ③ Because a localized pressure drop in the hydraulic circuit was found to be the cause of noise, the mechanism behind reduced noise could be verified using a relatively simple method of increasing the lubrication pressure.

These outcomes cannot be obtained using only an experimental approach, highlighting the usefulness of CFD.

6. References

- (1) Kazuo Suzuki, Takafumi Kawamura, Noriyuki Sasaki: Chapter 6 Cavitation, in Hull Resistance and Propulsion, Ship Marine Engineering Series 2, Seizando Publishing, (2012), pp.211-240
- (2) Masaru Shimada: "Elucidation of Noise Mechanism of Hydraulic System Using CFD," Proceedings of the 2024 Spring Meeting (Spring), pp. 1-4, 20245156, Reprinted with permission from the Society of Automotive Engineers of Japan, Inc.

■ Authors ■



Masaru SHIMADA

Method for Designing Lubricant Life

Yuma MOCHIZUKI* Gou KATOU** Makoto MAEDA*

Abstract

Lubricants degrade over time due to operating conditions and aging, leading to a loss of their initial performance. While degradation is known to accelerate with high lubricant temperatures and the presence of metal catalysts, no quantitative studies have been conducted to evaluate the impact of each factor on lubricant degradation. This paper presents degradation tests of lubricants, where lubricant temperature and the amount of metal catalysts were varied to quantitatively assess the effects of these factors on the remaining service life. The insights gained are valuable for the development of new lubricants and for planning optimal lubricant-change intervals.

1. Introduction

The function of additives in lubricants is to enhance the properties of the base oil and provide performance characteristics that the base oil alone does not offer, thereby improving the overall performance of the lubricant. In particular, transmission lubricants contain various additives that help control the friction characteristics of clutches, prevent the seizing of gears and other sliding parts, and improve durability. However, lubricants degrade over time and under specific operating conditions. Degradation refers to the change in the properties of lubricants, resulting in the loss of their initial performance. Because degradation can interfere with the operation of vehicle components or damage them, proper design of the lifespan of lubricants is crucial.

Lubricant is well known to deteriorate more rapidly at higher temperatures⁽¹⁾. Additionally, the presence of metal catalysts accelerates lubricant degradation⁽²⁾. In real-world scenarios, lubricants are used under conditions where both of these factors change in a complex manner. However, no quantitative studies have been reported on how each of these factors affects lubricant degradation.

This paper presents an investigation into the sensitivity of automotive transmission lubricants to lubricant temperature and the amount of metal catalysts. The study involved comparing lubricants degraded under various conditions by varying both the lubricant temperature and the amount of metal catalyst.

2. Experimental Methods

In transmission lubricants for automotive applications, the most significant effect of lubricant deterioration is the depletion of additives that control the friction characteristics of the clutch. As the lubricant deteriorates, issues such as shocks during clutch release and engagement become a concern⁽³⁾. To address this, our company mathematically estimates the remaining lifetime of the lubricant based on the depletion of additives that contribute to clutch friction characteristics. In this model, a value of 100 represents the lifetime of new lubricant, and 0 represents the lifetime of lubricant completely depleted due to degradation. In this paper, the remaining lubricant lifetime is used as an indicator of lubricant degradation.

*Innovative Technology Development Department **Hardware System Development Department

Table 1 ISOT Test Conditions

	Test 1	Test 2	Test 3	Test 4	Test 5	Test 6	Test 7	Test 8	Test 9	Test 10
Temperature, °C	50	80	110	110	120	140	140	160	175	180
Time, h	144	144	144	1,152	280	144	576	144	216	144

First, to determine the relationship between lubricant temperature and degradation rate, ISOT tests were conducted under the conditions listed in Table 1, and the remaining lifetime of the degraded lubricant was examined.

Existing AT lubricant was used. Next, the influence of metal catalysts was investigated by examining the remaining lifetime of lubricant samples that underwent the heating test without a metal catalyst (Table 2) and the unit-durability test (Table 3), which involved a significant amount of metal catalysts, such as unit components and their wear powder.

Table 2 Heating Test Conditions

	Test 1	Test 2	Test 3	Test 4
Temperature, °C	100	100	120	140
Time, h	1,000	3,000	3,000	2,000

Table 3 Unit Durability Test Conditions

	Test 1	Test 2	Test 3	Test 4
Driving Conditions	A	B	C	D
Distance, km	37,000	5,000	38,000	18,000

3. Results and Discussion

3.1 Relationship between lubricant temperature and degradation rate

Table 4 lists the results of the lubricant analysis after the ISOT tests. The reaction rates and rate constants were calculated based on the remaining lubricant lifetime.

To examine the relationship between lubricant temperature and degradation rate, the reaction rate constants are plotted starting from 110 °C, the temperature at which the progression of degradation was first observed.

Notably, when the temperature difference from 110 °C is x °C, the reaction rate multiplier is $e^{0.0471x}$ (Fig. 1).

By applying this analysis, the heat-damage level of lubricant exposed to 110 °C for 1 h can be defined as 1, which is considered the unit number for the magnitude of heat damage. This allows us to summarize the experiments conducted at different lubricant temperatures, as shown in Fig. 2.

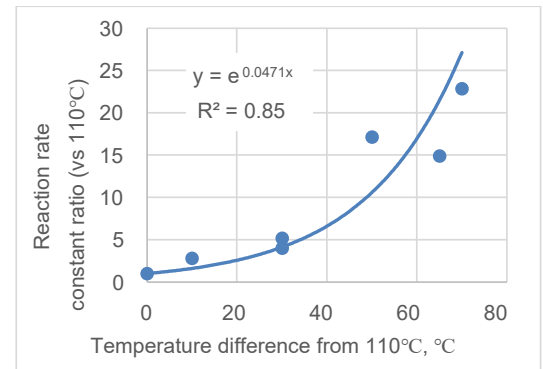


Fig. 1 Relationship between Lubricant Temperature and Reaction Rate Constant

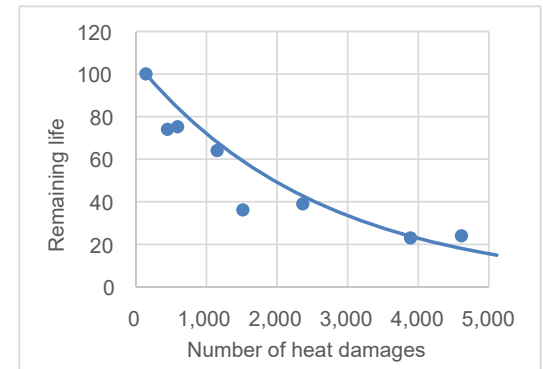


Fig. 2 Sorting Remaining Life Based on Number of Heat Damages

Table 4 Results of ISOT Test

	Test 1	Test 2	Test 3	Test 4	Test 5	Test 6	Test 7	Test 8	Test 9	Test 10
Remaining life	100	100	100	64	74	75	39	36	24	23
Reaction rate	0	0	0	0.031	0.093	0.172	0.106	0.444	0.352	0.535
Reaction rate constant	0	0	0	0.0004	0.0011	0.0020	0.0015	0.0065	0.0057	0.0087

3.2 Effect of metal catalysts

The remaining lubricant lifetime after each test was calculated and plotted against the number of heat damages (Fig. 3). The lubricant from the heating test without the metal catalyst exhibited a longer remaining lifetime compared to the lubricant from the ISOT test with the metal catalyst, despite experiencing the same number of heat damages.

In contrast, the lubricant containing a large amount of metal catalysts, such as unit components and their wear powder, exhibited a shorter remaining lifetime, indicating a higher degradation rate. Metal catalysts, such as iron and copper, are believed to accelerate the depletion of the additives.

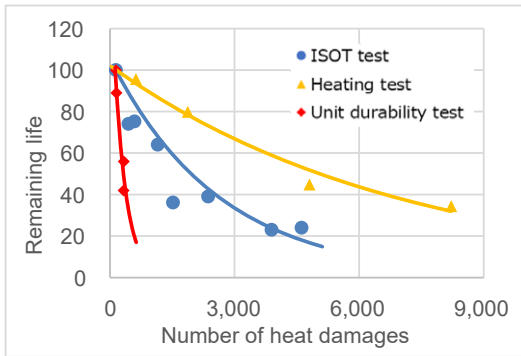


Fig. 3 Sorting Remaining Life
Based on Number of Heat Damages

3.3 Examination using multiple regression analysis

To calculate the degree of influence of each factor, a multiple regression analysis was performed on the results. The remaining lubricant lifetime served as the objective variable, the number of heat damages as the explanatory variable, and the amounts of iron and copper elements in the lubricant as the variables representing metal catalyst content. The obtained correlation coefficient was 0.83, indicating a strong correlation.

In Fig. 4, the horizontal axis represents the remaining lubricant lifetime, calculated using the prediction equation from the multiple regression analysis, while the vertical axis represents the remaining lubricant lifetime measured experimentally. The calculated values exhibited a strong correlation with the measured values, suggesting that the quantitative relationships between the duration of lubricant exposure at each temperature, the amount of metal catalysts, and lubricant degradation were successfully established.

The standardized partial regression coefficients for each factor were also compared. The results demonstrate that the strength of influence on lubricant degradation follows this order: number of heat damages, amount of copper in the lubricant, and amount of iron in the lubricant.

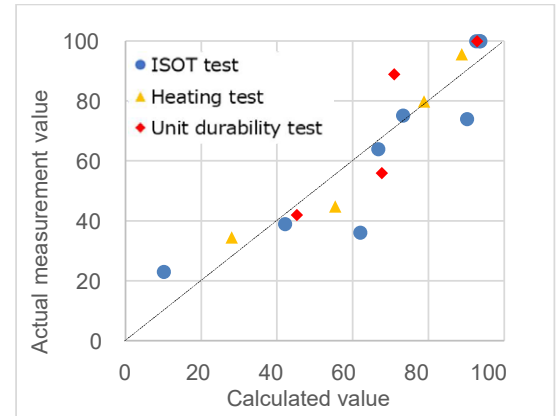


Fig. 4 Multiple Regression Analysis Results

4. Summary

The degradation of lubricants is influenced by metal catalysts as well as the duration for which the lubricant is subjected to various temperatures. By comparing the remaining lifetime of the lubricant after degradation under different conditions, the degree of influence of each factor was quantitatively determined.

The findings provide essential knowledge for designing new lubricants with a service life suitable for real operating environments, as well as for establishing an appropriate lubricant-change frequency. Future improvements include increasing the design accuracy of lubricant lifetime by considering the effects of local heat generation in the unit and the additive depletion due to lubricant adsorption on the sliding surfaces. This will help establish a more accurate design for lubricant lifetime under actual operating conditions.

5. References

- (1) Mitsuru Toyoguchi: On antioxidants for lubricating oils, *Synthetic Organic Chemistry*, 13, 11, 512–516 (1955).
- (2) Katayama: Oxidation of lubricating oil, *Journal of Oil Chemistry*, 5, 5, 261–270 (1956).
- (3) Toshihiko Ichihashi: Action of friction modifier on clutch and its degradation mechanism, *The Japan Petroleum Institute*, 41st Petroleum and Petrochemical Conference, 2F13 (2011).
- (4) Mochizuki, Kato, Maeda: Lubricant Life Design Method, *Proceedings of Tribology Conference Fall 2024 Nago*, 2024, A31

■ Authors ■



Yuma MOCHIZUKI



Gou KATOU



Makoto MAEDA

Technology to Restore the Performance of used CVT fluids by Adding Additives

Akira SUGIMURA* Gou KATOU* Makoto MAEDA**

Abstract

Fluids for continuously variable transmissions (CVTs) are designed by our company to be non-replaceable. However, under certain operating conditions, the additives can deplete significantly, causing shocks during the engagement and release of wet clutches. This study explored the mechanism of additive depletion and its impact on the performance of fluids. The insights gained were then used to develop more effective the additives.

The effectiveness of the additive agent was tested in actual vehicles. The results confirmed that supplementing the additives reduced the shocks and prolonged the improvement compared to fluid replacement. Additionally, no adverse side effects were observed. These findings highlight the significant potential of the additive in restoring CVT fluid performance.

1. Introduction

In recent years, as global environmental concerns have grown, reducing CO₂ emissions throughout the product lifecycle and supply chain has become a critical issue for achieving a low-carbon, recycling-oriented society.

The lubricating oil used in continuously variable transmissions (CVTs), called CVT oil, developed and manufactured by our company is designed to be “fill for life” and does not require replacement. However, under certain operating environments and conditions, some performance of CVT oils can deteriorate and necessitate replacement. The waste oil generated during this exchange is typically incinerated, releasing CO₂.

While research into lubricant regeneration technology is ongoing¹⁾, the CO₂ emissions resulting from energy consumption during the regeneration process have been identified as a new environmental concern.

Against this backdrop, restoring the degraded performance of the oil without replacing it is believed to reduce the amount of waste oil and, in turn, contribute to a low-carbon, recycling-oriented society. Consequently, we pursued the development of a technology to restore lubricant performance through additive supplementation.

2. Aims and objectives of this development

CVT oils are required to smoothly engage and release the wet clutch during forward and reverse shifts, as well as when the auxiliary gearbox shifts gears. However, if the oil deteriorates excessively, shocks may occur during engagement and release, leading to driver discomfort. The main cause of this issue is the depletion of CVT-oil additives, which most significantly impacts the friction property of the wet clutch (referred to as “wet clutch friction property”) ²⁾.

Despite oil degradation, other performance aspects, such as the friction property of metal parts, hydraulic performance, and cooling efficiency, remain sufficiently intact. When a degraded lubricant is replaced with fresh oil to restore wet clutch friction property, approximately 8 L of waste oil is generated. This creates a significant burden on customers in terms of replacement costs and work time.

*Hardware System Development Department **Innovative Technology Development Department

Therefore, the present study aimed to develop an additive that moderates the shocks while reducing both the amount of waste oil and the customer burden by diluting the necessary additive to restore wet clutch friction property with base oil and adding it to the CVT oil.

The main technical objectives in this development are as follows.

Objective 1: The goal is to moderate shocks during the engagement and release of wet clutches and to ensure that the improvement (referred to as “durability”) lasts as long as it would with a full oil replacement.

Objective 2: To prevent any impact on the friction property of metal components such as belts and pulleys (hereinafter referred to as Steel-on-steel friction property).

Objective 3: To avoid affecting the performance of CVT oil, even when additives are supplemented in excess of the prescribed amount or the amount in the fresh oil.

3. Consideration in solution methods

The types and amounts of the additives were examined by summarizing their functions (Table 1).

Table 1 Main functions of additives

Additives	Function
Friction modifier	Wet clutch friction adjustment
	Steel-on-steel friction adjustment
Detergent dispersant	Disperses contamination
	Neutralize any acid contents
	Wet clutch friction adjustment
	Steel-on-steel friction adjustment
Extreme-pressure additive	Steel-on-steel friction adjustment
	Prevents wear and seizure
Anti-oxidant	Prevents oxidation
Viscosity index improver	Viscosity index adjustment

Solution approach to objective 1

The mechanism of additive depletion is that the oxidized degradation products of the base oil, which are generated by the sliding heat of the components³⁾, trap the additives and deplete them. Specifically, the detergent dispersant and friction modifier (hereinafter referred to as “FM”), which control the formation of oxidized degradation products and wet clutch friction property, are consumed. Therefore, additives must be added to compensate for this depletion.

However, the formation of oxidized degradation products is accelerated by the catalytic effect of metal ions generated by the sliding of the unit components during driving⁴⁾. Therefore, to ensure that the durability is equivalent to that in the case where the oil is replaced with fresh oil, considering this effect is necessary to determine the amount of detergent dispersant to be added.

Solution approach to objective 2

In a lubricating environment where the steel-on-steel friction property is present, the temperature of the sliding surface is high. This condition activates the Brownian motion of FM with low molecular weights, making the adsorption of the FM onto the metal surface difficult.

However, if the FM is present in larger amounts than the extreme-pressure additive that controls the steel-on-steel friction property, the FM is adsorbed on the metal surface, thereby reducing the steel-on-steel friction. Therefore, the ratio of the extreme-pressure additive to the FM must be considered when determining the amount to be added.

Solution approach to objective 3

When additives are supplemented in excess of the prescribed amount or the amount in the fresh oil, the amount of additives in the oil becomes excessive. However, the state in which additives are adsorbed on metal surfaces is determined by the ratio of the additives present. Therefore, if the ratio of the additives in the supplementing agent can be optimized, the performance of the oil can be similar to that of the fresh oil, even if the additive is added to the fresh oil.

The amount of each additive agent was determined as follows: First, the oil with the greatest amount of additive depletion was selected from the recovered oils and those that had completed the durability tests, and was used as the used oil. The additive agents were designed such that, after being added to the used oil, the oil performance would be restored, and its durability would become equivalent to that of fresh oil after an oil change. Subsequently, the amount of the FM was determined by applying a safety factor to the amount required for the used oil. The amount of detergent dispersant was adjusted to match the detergency property of the fresh oil when added to the used oil. Next, the detergent dispersant and FM were added to the fresh oil to create an oil with excess amounts of FM and detergent dispersants. Finally, the amount of the extreme-pressure additive was adjusted through preliminary experiments to obtain the condition where the steel-on-steel friction property was equivalent to that of the fresh oil.

4. Confirmation of effectiveness

The detergency property (test method: JPI-5S-55-99), wet clutch friction property (test method: JASO M349), and steel-on-steel friction property (test method: JASO M358) were examined using CVT oil (fresh oil) and used oil before and after the addition of additive agents.

4.1 Confirmation for objectives 1 and 2

The detergency property and wet clutch friction property of the used oil after additive treatment were comparable to those of fresh oil, and the durability was restored to a level exceeding that of fresh oil (Figs. 1, 2, and 3). Additionally, the steel-on-steel friction property was also comparable to that of fresh oil (Fig. 4).

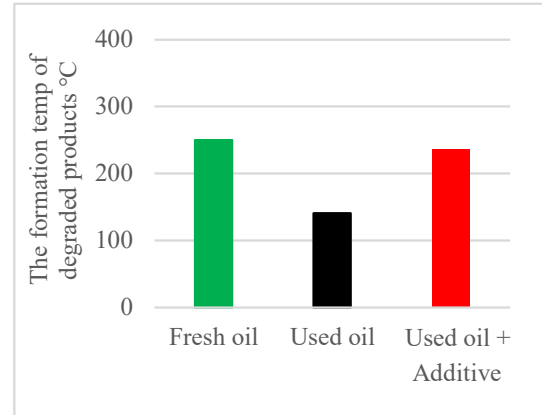


Fig. 1 Detergency test results

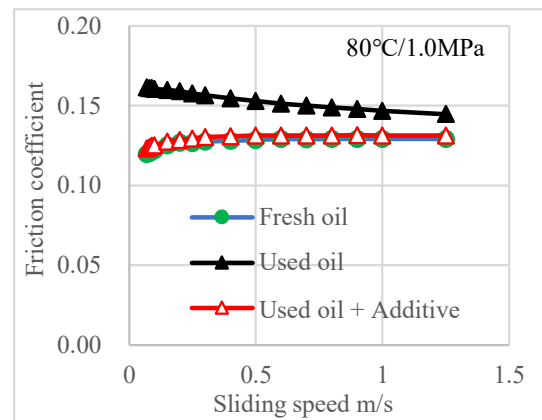


Fig. 2 Wet clutch friction test results

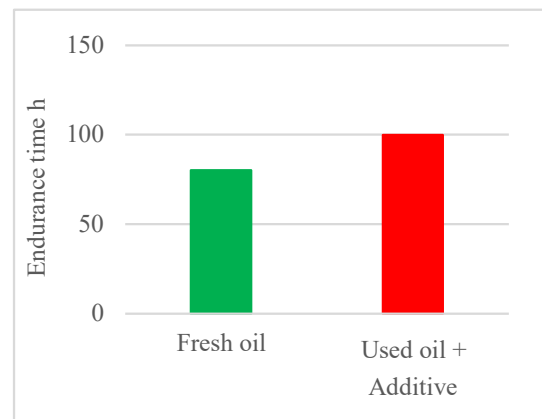


Fig. 3 Wet clutch friction endurance test results

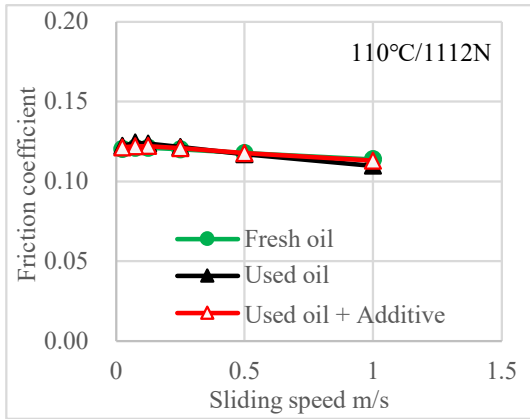


Fig. 4 Steel-on-steel friction test results

4.2 Confirmation for objective 3

The wet clutch friction property and steel-on-steel friction property were comparable to those of the fresh oil, even when the fresh oil was added to the agents (Figs. 5 and 6). The other performances were comparable to those of the fresh oil.

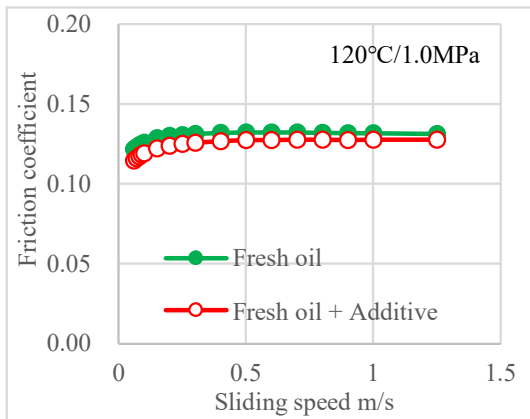


Fig. 5 Wet clutch friction test results

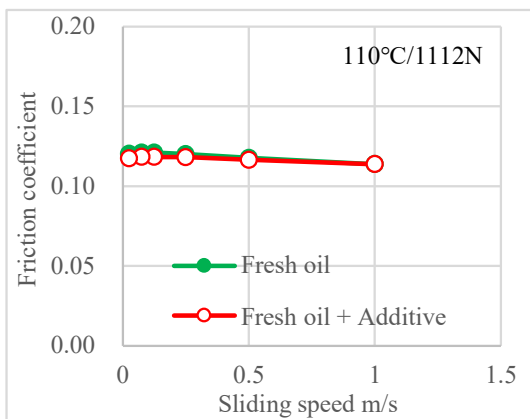


Fig. 6 Steel-on-steel friction test results

5. Verification using actual vehicle

Driving tests were conducted under conditions that accelerated CVT oil degradation, inducing shocks during wet clutch engagement and release. After shocks occurred, the agent was added to the oil, and the additive supplementation was confirmed to reduce the shocks. Continued driving tests demonstrated that the distance between shocks was longer than that with a fresh oil change.

The agent was added again, and further driving was conducted until the next shock occurred. These results confirmed that the effects and durability of the additives were reproducible. Additionally, multiple applications of the agent had no negative impact (such as seizure, wear, or damage) on the performance of the CVT unit (oil pressure, gear shift performance) or any of its components.

6. Summary

The present study developed an additive agent that moderates shocks during the engagement and release of wet clutches and has longer durability than that of a fresh oil change.

By adding the newly developed agent to our CVT oil, its performance can be repeatedly restored without compromising the overall effectiveness of the oil. Furthermore, the use of this agent reduces the amount of waste oil to just 0.5 L, significantly lowering the environmental burden compared to traditional oil changes.

The method of recovering oil performance using the additive agent developed in this study is an effective approach for realizing a low-carbon and recycling-oriented society, thus significantly contributing to the improvement of lubricant design technology.

7. References

- 1) Okubo, Yano, et al.: Development of Lubricant Life Extension/Regeneration Technology that Contributes to a Low-Carbon, Recycling-Oriented Society, Mitsubishi Heavy Industries Technical Review Vol. 61 No. 1 (2024).
- 2) Ichihashi: Action of friction modifier on clutch and its degradation mechanism, Japan Petroleum Institute, 41st Annual Meeting of Japan Petroleum and Petrochemical Society, (2011) 2F13.
- 3) Toyoguchi: On antioxidants for lubricating oil, Organic Synthetic Chemistry, 13, 11 (1955) 512–516.
- 4) Mochizuki, Kato, Maeda: Method for Designing Lubricant Life, Proceedings of Tribology Conference Fall 2024 Nago, 2024, A31.

■ Authors ■



Akira SUGIMURA



Gou KATOU



Makoto MAEDA

Design concept and technical verification of low viscosity reducer oil

Kazunori ISHIGAMI* Gou KATOU* Makoto MAEDA**
Ryo SASAKI*** Hitoshi KOMATSUBARA***

Abstract

The development of electric vehicles (EVs) is accelerating in response to the urgent need to curb CO₂ emissions and combat global warming. However, increasing battery capacity to ensure a sufficient driving range significantly increases manufacturing costs. This study aims to reduce the necessary battery capacity by lowering electric power consumption in EVs. To achieve this, a low-viscosity oil for reduction gears was developed, and its performance was evaluated. Specifically, the study focused on friction (agitation resistance) in the reduction gears, designed low-viscosity oil to reduce power consumption, and verified its performance through in-life tests. The results confirmed that the developed low-viscosity oil significantly reduced friction in the reduction gears compared to conventional oil, leading to lower power consumption. This low-viscosity oil effectively improves the electric power efficiency of EVs and is expected to contribute to reducing battery costs.

1. Introduction

In recent years, as global regulations on CO₂ emissions have tightened to combat climate change, the automotive industry has accelerated electrification. Alongside traditional internal combustion engine vehicles, automakers and suppliers are focusing their efforts on developing and promoting hybrid electric vehicles (HEVs) and battery electric vehicles (BEVs). However, a significant challenge to the widespread adoption of BEVs is the limited driving range. Extending the range requires increasing battery capacity, which significantly raises costs. Therefore, improving energy efficiency (hereafter referred to as 'energy saving') is a critical solution to this issue.

Additionally, to meet the demand for smaller, more powerful EVs, drive systems that combine small-diameter, high-revolution motors with high reduction-ratio gears are becoming mainstream¹⁾. With the adoption of such high-power-density motors, addressing motor heat generation has become a new technological challenge, and motor-oil cooling systems are gaining attention as an effective solution.

This study focuses on reducing torque loss (friction reduction) in reduction gears to lower electric power consumption in EVs. As part of this effort, a low-viscosity reducer oil suitable for motor oil cooling was developed. This paper presents the design concept and verification results of the new oil.

2. Development aims and objectives

The aim was to create the lowest viscosity oil among all the benchmark oils in order to reduce electricity consumption, while also achieving better performance than conventional oils (ATF) in terms of friction characteristics during sliding, fatigue prevention of metal parts, and anti-seizing performance.

*Hardware System Development Department **Innovative Technology Development Department ***ENEOS Corporation



3. Issues with low viscosity

The Stribeck curve in Fig. 2 demonstrates that, in the fluid lubrication range, the low-viscosity ATF has a lower coefficient of friction compared to conventional oils. However, in the mixed lubrication range, the oil film becomes thinner, making metal contact more likely. This can lead to an increase in the coefficient of friction and a decrease in the anti-fatigue and anti-seizing performance of the metal.

Conventional low-viscosity technologies have prevented metal contact (improved extreme pressure) by blending highly viscous oil-film-forming polymers to ensure the formation of an oil film²⁾. However, to achieve the target viscosity, these polymers, which have a thickening effect, were excluded from this development.



4. Design concept

To prevent metal contact in the mixed lubrication zone caused by low viscosity, extreme pressure needs to be enhanced by forming an additive film. This was achieved by utilizing the heat generated from the thinning oil film to rapidly form adsorption and reaction films on the sliding surfaces³⁾. Two phosphorus-based additives with distinct properties were blended to quickly create protective films in the mixed lubrication zone.

5. Improvement of extreme-pressure performance

5.1 Blending of phosphorus additives

To mitigate rapid load fluctuations in reduction gears, preventing metal contact between the sliding parts by forming a protective film as early as possible in the mixed lubrication zone is crucial. A strategy was developed in which an adsorption-type phosphorus additive forms a film on the sliding surfaces under low surface pressure and low-speed conditions, while a chemical-reaction-type phosphorus additive creates a film under high surface pressure and high-speed conditions.

5.2 Revision of additive formulation

Considering the performance requirements⁴⁾ of the reducers outlined in Table 1, the additive formulation was revised from existing oils to ensure both extreme pressure and electrical insulation properties, while addressing the challenge of low viscosity. The revision aimed to eliminate unnecessary additives from the reducer oil to maximize the formation of a reactive film on the sliding surfaces. Specifically, dispersants and friction modifiers, which affected the friction characteristics of the wet clutches, were removed.

Table 1 Performance Required for e-Axle

Performance required for e-Axle (Reducer)	Performance required for Oil	Objectives of additive formulation optimization
Reduction of agitation resistance	Low viscosity	Elimination and reduction of dispersants with thickening effects, FM agents
Oil-cooling the motor	Electrical insulation	Elimination and reduction of conductive dispersants and FM agents
Gear durability	Wear resistance, Pitching resistance, Scuffing resistance	To maximize the effectiveness of the two phosphorus-based additives, the dispersant and FM agent that cause competitive adsorption reduced or eliminated

6. Verification results

The friction and anti-seizing performances of the developed oil were compared with those of the conventional oil and low-viscosity ATF. The results are discussed below.

6.1 Friction coefficient

Friction coefficient measurements were conducted under the mixed lubrication conditions specified in Table 2 using the mini traction machine (MTM) test. The results, shown in Fig. 3, indicate that the newly developed oil has a lower coefficient of friction compared to the low-viscosity ATF. These results validate the design concept, confirming that the adsorbed and chemically reacted phosphorus additives form adsorption and reaction films on the sliding surfaces, preventing metal contact and resulting in reduced friction.

Table 2 MTM test conditions

Surface pressure[GPa]	1.2(Load 60N)
Speed[mm/s]	10-3000
Oil temperature[°C]	40
Slip ratio[%]	50

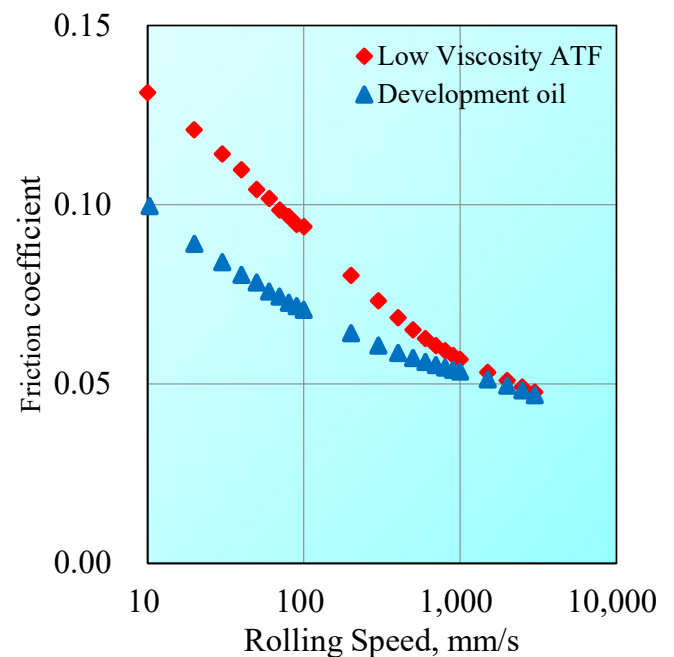


Fig. 3 MTM test

6.2 Anti-seizing performance

Figure 4 presents the evaluation results of the anti-seizing performance in a high-speed four-ball test. When the conventional ATF was replaced with low-viscosity ATF, the maximum non-seizing load decreased compared to the existing oil. However, the maximum non-seizing load of the newly developed oil was higher than that of the conventional ATF, as predicted by the design concept. These results validate the design concept, where the additive formulation was revised to form a reactive film on the sliding surface.

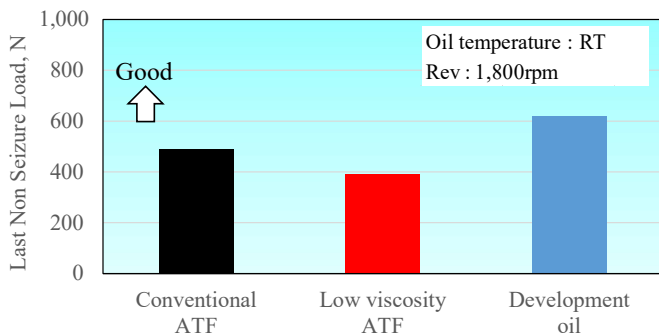


Fig. 4 High-speed 4-ball test

6.3 Assessment of seizure resistance under assumed conditions of actual gears

The anti-seizing performance of the developed oil was compared to that of the existing oil using high-peripheral-speed gears under test conditions simulating a poorly lubricated environment on the gear fracture surface and the running pattern of a vehicle (Fig. 5). The developed oil demonstrated superior resistance to seizure, with the rotational speed at which surface damage occurred being higher than that of the conventional ATF, particularly under conditions simulating BEV start-up running (high torque).

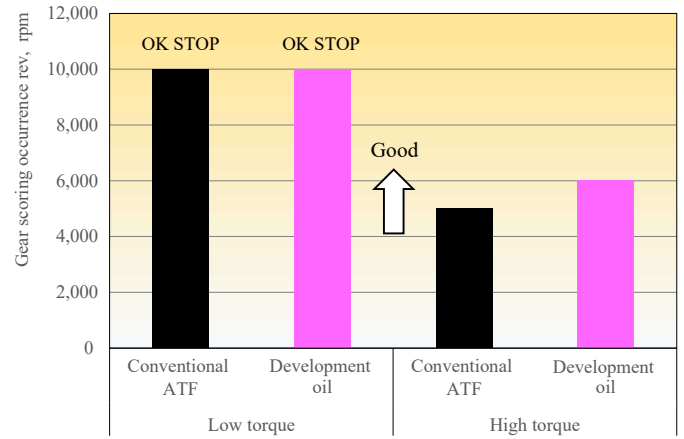


Fig. 5 High-speed gear seizure test

7. Summary

In this study, a reduction gear oil for electric vehicles was developed, yielding the following results:

The newly developed reduction gear oil demonstrated industry-leading low-viscosity characteristics while offering excellent friction properties, anti-fatigue performance, and anti-seizing performance during gear component sliding. Additionally, the oil provided the required electrical insulation for motor oil cooling.

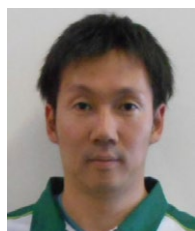
Performance evaluation tests confirmed that the newly developed oil improved energy efficiency by approximately 10% compared to conventional oils. This efficiency improvement is expected to directly contribute to extending the driving range of electric vehicles.

The findings from this study will help address technical challenges in the promotion of electric vehicles and will make a significant contribution to advancing lubricant design technology in the future.

8. References

- 1) Tsukagoshi, et al: Development of Synchronous 3-Pulse Control in High-RPM Motors for e-Axle, Journal of Society of Automotive Engineers of Japan, Vol. 53, No. 3, May 2022
- 2) Masuda: Development of ultra-low viscosity ATF, JXTG Technical Review, Vol. 61 (2019.7)
- 3) Ariyama, Komatsubara: Elucidation of Friction Reduction Mechanism of Low Viscosity Differential Gear Oil, Tribology Conference (Fall 2017)
- 4) Ishigami, Arakawa, Maeda: History and Latest Trends in Automotive Transmission Oils, Tribologists (2020)
- 5) Ishigami, Kato, Maeda: Design Concept of Low Viscosity Reduction Gear Oil and Its Verification, Proceedings of Tribology Conference 2024 Fall Nago, 2024, A32

■ Authors ■



Kazunori ISHIGAMI



Gou KATOU



Makoto MAEDA

Innovation in the development of CVT unit systems and their applications in projects

Takeshi KANEDA* Toru YOKOTA**

Abstract

As the demands for automobile performance increase, the requirements for the development of CVT units are becoming more complex. In addition, many tradeoffs are involved in their development, making it difficult for development to proceed without rework. In response to these challenges, JATCO established a system architecture analysis method that applies Quality Function Deployment⁽¹⁾.

This report describes the issues that were identified in the application of the method to actual projects to complete development and the measures taken against the issues.

1. Introduction

In recent years, the requirements for the development of new CVT units have become increasingly diverse and complex owing to the need for more compact units to meet stricter vehicle crash safety requirements as well as the increased demand for improved exhaust emissions and fuel consumption. Under these circumstances, smooth development using conventional methods has become difficult. To address this situation, we introduced a systems engineering (SE) method⁽²⁾ to perform development with a holistic view of the entire vehicle, powertrain, and CVT, thereby realizing a smooth development process with no rework and successfully achieving mass production. This report provides an example.

2. Issues identified when the method is applied to actual projects

For the smooth development of a new CVT unit, it is necessary to follow the V-process of SE. In particular, the first process, that is, system design, in which vehicle requirements are translated into unit requirements, is important, and its success or failure affects all downstream processes (Fig. 1). Therefore, the key points for high-quality development are whether all issues can be identified without omission and to clearly allocate requirements in the design review, which is the final step in the system design process.

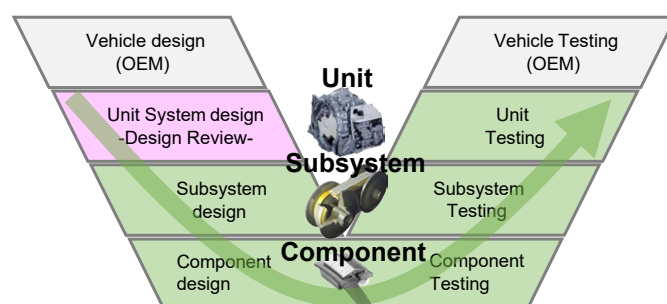


Fig. 1 V-shaped development process

*Unit System Development Department **Innovative Technology Development Department

In the system design stage, it is important to consider a set of processes to identify changes, extract issues, examine issues, and review the design (Fig. 2).

The following section describes the issues that arise in each process and their solutions when applying a requirements traceability matrix to a real project.

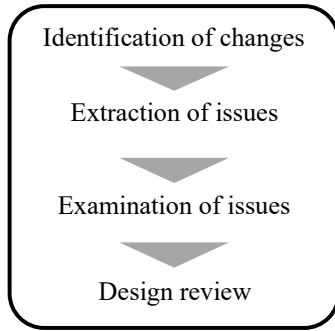


Fig. 2 The system design process until the design review

2.1 Identification of changes

Identifying changes is an important step when conducting projects. By utilizing the requirements traceability matrix, it is possible to ensure the completeness of the list of requirement items, assuming that the changes, which are the input information (customer requirements), are clearly identified. However, the following issues arose in its application to actual projects.

2.1.1 Issues in understanding requirements

There were cases in which, among the customer requirements, some requirement items were missing or the values of some requirements were unspecified. These issues were overcome by introducing a requirement management tool, setting out the company's in-house performance requirement items that were necessary for development, and having the customer present the target values for these requirement items, thereby preventing missing requirement items. Additionally, misunderstandings arising from a lack of communication were prevented by creating records of the agreed-upon parties as well as the dates and times of agreements.

To allocate vehicle requirements to unit requirements and unit requirements to subsystem requirements, a planning drawing framework (Fig. 3) was developed, and requirements–function–logic (RFL) at each level was managed using planning drawings, thereby preventing unclear allocations.

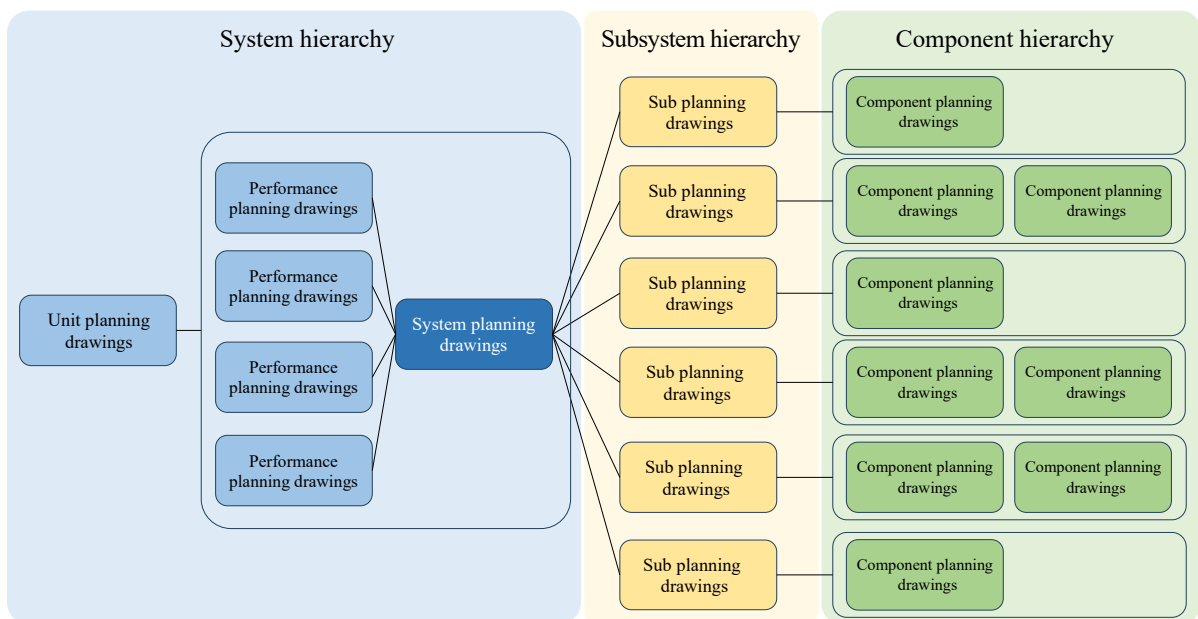


Fig. 3 The framework of planning drawings

2.1.2 Issues in understanding specifications

In the early development stages, it was easy to identify changes because the specifications were determined based on the performance requirements. However, specifications are frequently changed in later development stages to meet production requirements, supplier requirements, cost targets, and weight targets, making it less easy to identify all changes. To solve this problem, a drawing-based change identification and listing system was introduced into the drawing-release process, and a process gate was added to check for changes (Fig. 4).

2.2 Extraction of issues related to changes

By utilizing the requirements traceability matrix, it was possible to extract all impacts of the changes. This made it possible to efficiently extract the issues raised by experts and avoid any issues caused by variations in individual abilities. However, the following issues became apparent during the actual application of the project.

2.2.1 Insufficient issue extraction owing to delays in updating information

The extraction of issues in the requirements traceability matrix was based on the existing CVT system configuration, and it was not always possible to cover all issues, owing to delays in updating information, such as issues associated with the introduction of new systems and the horizontal deployment of specification changes in other models.

In response, a process (Fig. 5) was introduced to examine whether issues should be added based on the latest information in each functional design using the items extracted from the changes and the requirements traceability matrix as a base. This process prevented any issues from being overlooked and enabled the regular updating of the requirements traceability matrix.

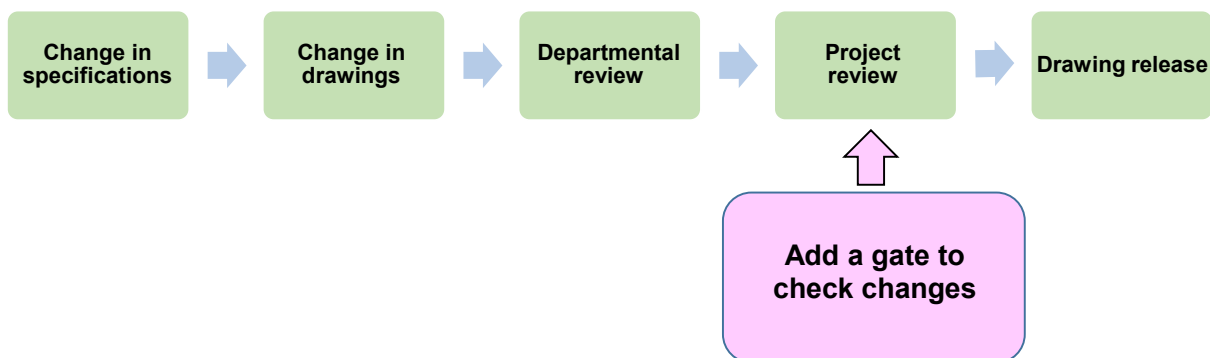


Fig. 4 Improving the drawing process

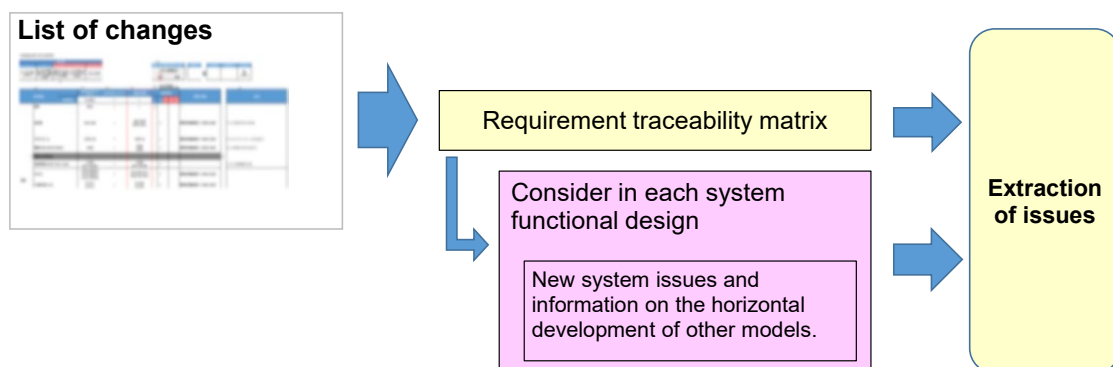


Fig. 5 The issue extraction process

2.2.2 Overextraction of issues

The requirements traceability matrix was designed to allow for the extraction of all items that might be generally affected so that no issues would be missed. This resulted in a significant number of extracted items, and there was a concern that the resources required for the subsequent examination of these issues would be excessive. In response to this concern, the changes extracted from the requirements traceability matrix were assessed by each design department, and if they were judged to have no obvious impact on the performance, they were excluded. This approach prevents an unreasonable increase in the number of items extracted from the matrix, thereby allowing time for the examination of important issues.

2.3 Examination of issues

The extracted issues were examined for each functional design, and the specifications were determined. At this point, requirement mediation was necessary for tradeoffs between functions, and substantial rework occurred when the specifications were not determined in an appropriate order.

The requirements traceability matrix was used to factor in the sequential order of design (extraction of key specifications), visualize the tradeoffs, and numerically evaluate the complexity of the system architecture (interface score). This approach clarifies the priorities of the functions and efficiently resolves tradeoffs.

Specifically, the tradeoff requirements for the changes were identified, and their complexity was quantified to enable a comparison with other changes. In addition, the issues were examined according to their priority, which was determined by evaluating them using the complexity and magnitude of the impact on key specifications and the unit layout on two axes, thus enabling the efficient resolution of complex tradeoffs (Fig. 6).

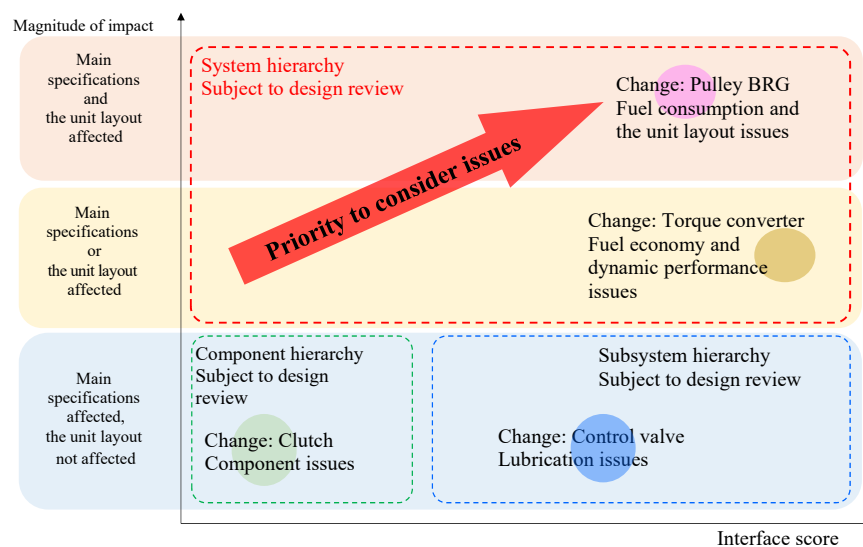


Fig. 6 Implementation of an Interface Score (Priority of issue study)

2.4 Review of issue examination

In this project, A level of meeting was assigned based on the presence of system issues extracted from the requirements traceability matrix, evaluation of the interface score, and magnitude of the impact on main specifications and the unit layout. This allowed us to focus on the most important issues (Fig. 7).

2.5 Examples of applications in actual project development

Five examples of project development applications are described below (Fig. 8).

- (1) During the development process, a major specification change occurred in the belt, which is a key component of the CVT.
- (2) In response to (1), the system issues were extracted. Based on the requirements traceability matrix, it was decided that fuel efficiency and dynamics (Wide-open-throttle start), which are the most important issues and have a high potential to affect the unit layout, would be addressed as priority 1 and that other issues would be addressed after the fuel efficiency and dynamic performance were resolved.

- (3) The ratio coverage must be expanded to ensure fuel economy and dynamic performance. To expand the coverage ratio, it was necessary to change the design of the pulley, which is another key component of the CVT.
- (4) System issues were extracted based on (3). Based on the requirements traceability matrix and other issues from (2) + prioritization, the durability of the pulley strength was reassigned as the new priority 1, and the unit layout, dynamics (highest speed), and operability issues were reassigned as the new priority 2.
- (5) A level of meeting was determined according to the magnitude of the impact of the system on the issues identified in (4).

The above approach makes it possible to focus on the necessary review processes, depending on the importance of the issues in the project.

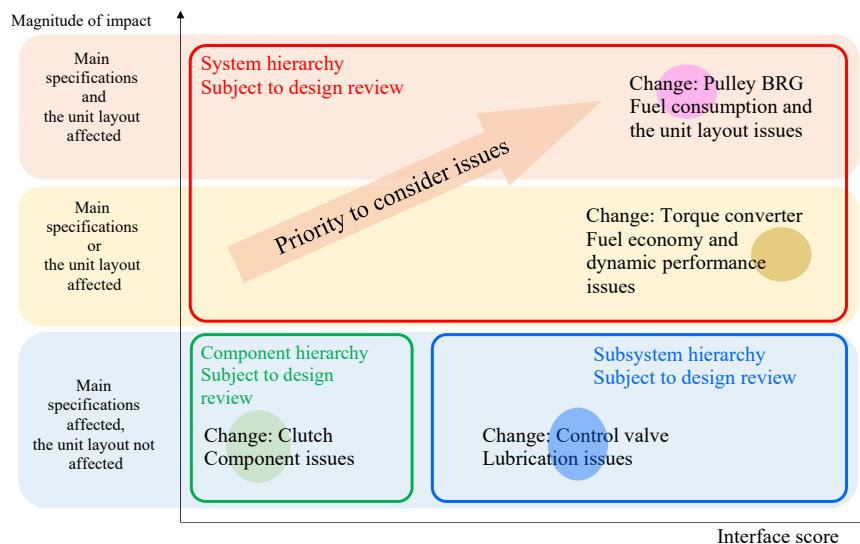
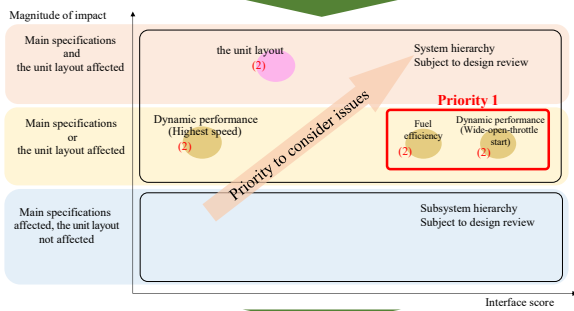


Fig. 7 Implementation of an Interface Score (Decide review level)

(2): System issue extraction in response to (1)

CVT basic specification	Requirements		Correlation						
	Ratio coverage	(1) Change	Contradiction	Contradiction	Contradiction	Contradiction	Contradiction	Advantageous	
	Lowest Ratio	(1) Change	Contradiction	Contradiction	Contradiction	Contradiction	Contradiction	Advantageous	
	Highest Ratio	(1) Change	Contradiction	Contradiction	Contradiction	Contradiction	Contradiction	Advantageous	
	Pulley pressure receiving area								
	Pulley shaft diameter								



(4): Extraction of system issues in response to (3)

CVT basic specification	Requirements		Correlation						
	Ratio coverage	(3) Change	Advantageous	Advantageous	Advantageous	Advantageous	Advantageous	Advantageous	
	Lowest Ratio	(3) Change	Contradiction	Advantageous	Advantageous	Advantageous	Contradiction	Advantageous	
	Highest Ratio	(3) Change	Contradiction	Advantageous	Advantageous	Advantageous	Advantageous	Advantageous	
	Pulley pressure receiving area	(3) Change							
	Pulley shaft diameter	(3) Change	Contradiction	Advantageous	Advantageous	Advantageous	Advantageous	Advantageous	

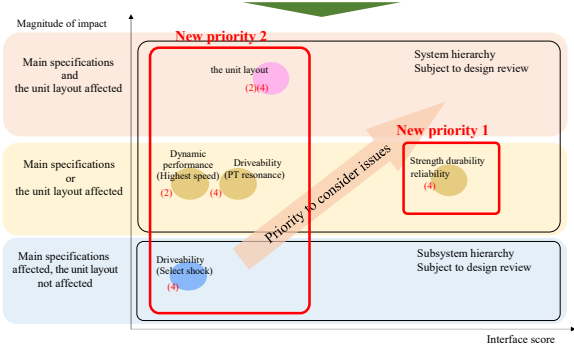


Fig. 8 Case study of project application

3. Outcome of the innovation in the system review

By applying the method described in this paper, the project contributed to the acquisition of the NCAP 5-star for an applicable car model by downsizing the unit size. This method also enabled the expansion of the ratio coverage, which contributed to improved fuel efficiency and dynamic performance by 13%, compared with those of the previous model (Fig. 9).

In addition, the development costs were reduced by approximately 14%, compared with those of the previous model.

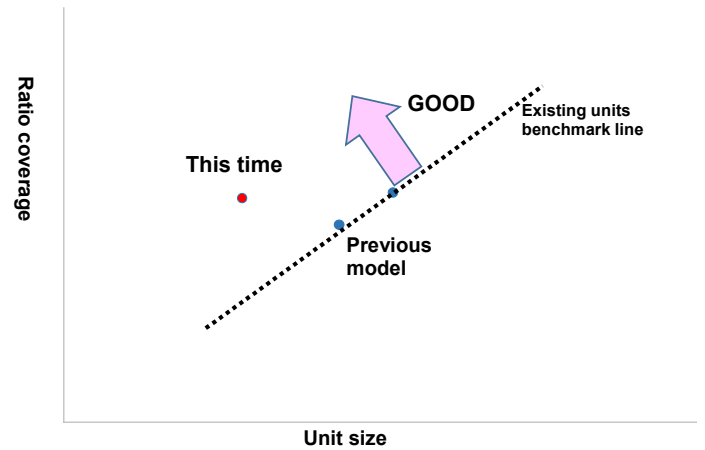


Fig. 9 Ratio coverage vs. Unit size

4. Discussion

This study describes an innovative method for developing CVT systems. In the future, to further improve quality, the application of this method will be expanded as follows.

4.1 Application to the development of electrification units

Although the system is not as complex as a CVT, it is necessary to develop one that encompasses not only the reduction gear but also the prime mover. Because the tradeoffs with vehicles will further increase, the present method can be used to achieve efficient and high-quality development.

However, it is also important to improve the accuracy of the requirements traceability matrix and create an environment in which the requirements traceability matrix can be visualized and discussed among the parties involved.

4.2. Application to the development of AT and CVT units

In the development of existing AT and CVT units, there are many system issues, such as recent regulations and the addition of new devices. The proposed method enables the efficient development of a wide variety of applications.

4.3. Cultivation of system human resources

As Japan's birth rate declines and its population ages, it is becoming increasingly difficult to pass on technology and cultivate human resources through on-the-job training, as was done in the past. By applying the proposed method, even inexperienced engineers can identify system issues and prioritize them, thereby enabling early human resource development.

5. Summary

This paper presents a case study of the application of the requirements traceability matrix to a project and discusses issues and their solutions in each process (Table 1).

The use of the requirements traceability matrix made it possible to prevent project issues from being overlooked and develop highly efficient and high-quality units.

Table 1 Issues and solutions in each process

Process	Issue	Solution
Identification of changes	Understanding of requirements	<ul style="list-style-type: none"> Requirement management tool Framework of planning drawing RFL
	Understanding of specifications	<ul style="list-style-type: none"> Identifications of changes based on drawings, listing Addition of a process gate to the drawing release process (check for changes)
Issue extraction	Insufficient issue extraction owing to delays in updating information	Process for considering whether or not to add an issue
	Overextraction of issues	Performance impact assessment process
Examination of issues	Rework owing to tradeoffs between functions	Prioritized by complexity and impact on key specifications and the unit layout
Design review	Review of issue examination	Assigning a level of meeting for the examination of extracted issues

6. References

- (1) Fuyuku Katsu and Yasushi Hattori, "Implementation of a system architecture analysis method in the automotive transmission development process," JATCO Technical Review No. 19 (2020).
- (2) Takashi Nakazawa, "New Engine Development Using Systems Engineering," Journal of the Japan Society of Mechanical Engineers, Vol. 119, No. 1177 (2016).

■ Authors ■



Takeshi KANEDA



Toru YOKOTA

Introducing the Jatco CVT-XS (JF023E) for Nissan KICKS

The “KICKS,” launched in North America by Nissan Motor Co., Ltd. in August 2024, is equipped with the Jatco CVT-XS (JF023E). The JF023E, which has been installed in the “Sentra” since October 2023, features a completely redesigned hydraulic system coupled with twin oil pump system, and multi-plate lock-up system using a three-way linear solenoid. These advanced mechanisms enhance the sense of power and driving performance. The ratio coverage is enlarged by reducing minimal belt pitch diameter, which contributes to improve fuel efficiency. Additionally, the vertical arrangement of the control valve assembly enabled very compact packaging dimensions and enhances safety in crash situations. The refined performance of the KICKS, enabled by its integration with the JF023E, has earned high praise from customers.

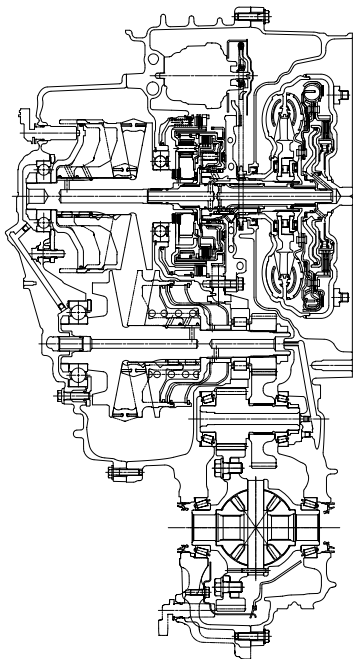


Fig. 1 Main cross-sectional view

Table 1 Specifications of JF023E

Torque capacity	280 Nm
Torque converter size	230 mm
Pulley ratios	2.805 - 0.357
Ratio coverage	7.9
Reverse gear ratio	0.745
Final gear ratio	5.341
Selector positions	P, R, N, D, B
Gear box length	379.9 mm
Weight (wet)	94.6 kg

KICKS



Introducing the JR913E 9-speed AT for INFINITI QX80, Nissan ARMADA and NISSAN PATROL

INFINITI QX80, launched in July 2024, is equipped with the JR913E 9-speed FR Automatic transmission. The JR913E offers approximately 40% wider gear ratios compared to the previous 7-speed AT. This, coupled with a newly developed 3.5L twin-turbo engine, results in improved acceleration response and fuel efficiency at high speed driving. Also, the direct hydraulic control system provides a more direct feeling during gear shifts.

NISSAN ARMADA and PATROL feature a terrain mode within their drive mode settings, enabling high-quality driving performance across various terrains, from urban areas to rugged off-road landscapes.

These vehicles utilizing the JR913E have achieved enhanced drivability and improved fuel efficiency, earning high praise from customers.

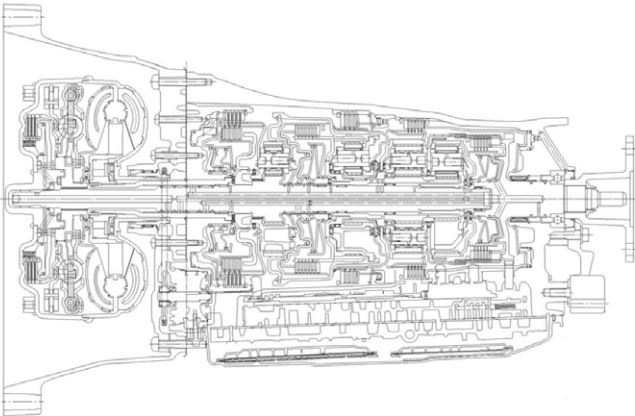


Fig. 1 Main cross-sectional view

Table 1 Specifications of JR913E

Torque capacity	700 Nm	
Torque converter size	260 mm	
Gear ratios	1st	5.425
	2nd	3.263
	3rd	2.249
	4th	1.649
	5th	1.221
	6th	1.000
	7th	0.861
	8th	0.713
	9th	0.596
	Rev.	4.799
Ratio coverage	9.1	
Final gear ratio (reference)	3.357	
Selector positions	P, R, N, D, +Manual shift (Paddle) (Park & Shift by wire)	
Overall length	439.5 mm	
Weight (wet)	100.5 kg	

QX80

ARMADA

PATROL



Introducing Shift Pulley for BRP-Rotax ATV transmission

Bombardier Recreational Products (BRP) is one of the top manufacturers of recreational vehicles, including all-terrain vehicles (ATVs) and personal watercraft (PWCs). JATCO has begun supplying pulleys for ATV transmissions to BRP-Rotax GmbH & Co KG, an Austrian company that manufactures powertrains for BRP. By leveraging the technology we have developed through our experience in the design and production of continuously variable transmissions (CVTs) for automobiles, we have opened the door to offering our products to off-highway mobility users. This component is produced at JATCO Mexico S.A. (JMEX).

Pulleys for ATV transmissions



POWER TRANSMISSION DEVICE

This patent relates to the vertical arrangement of the control valve as introduced in the product introduction “Introducing the Jatco CVT-XS (JF023E) for Nissan KICKS”.

1. POWER TRANSMISSION DEVICE

(Fig. 1)

Application Number :2024-509224

Application Date :23.3,2023

Patent Number :7596055

Registration Date :29.11,2024

Title :POWER TRANSMISSION
DEVICE

Inventors :Katsunori YAMASHITA,
Hirohisa YUKAWA,
Masahiro KOUYA,
Tomoo IKEDA, Kenji KOJIMA,
Akira HIGASHIYAMA,
Yasuaki YUMOTO,
Tsutomu ITOU,
Kazuya NUMATA,
Junnosuke KAWAHARA,
Kazunori AKIYAMA

【SUMMARY OF THE INVENTION】

[Problem] To dispose of two pumps in a housing without increasing the size of a power transmission device in the rotational axis direction.

[Solution] A power transmission device for a vehicle, comprising a housing that houses a power transmission mechanism, a control valve that controls the hydraulic pressure supplied to the power transmission mechanism, and a mechanical pump and an electric pump that supply oil to the control valve. The housing has a first chamber that houses the power transmission mechanism and the mechanical pump, and a second chamber disposed adjacent to the first chamber in a horizontal line

direction. The mechanical pump is disposed in the first chamber such that the rotational axis of the mechanical pump is oriented along the rotational axis of the power transmission mechanism. The control valve is disposed vertically in the second chamber, and the electric pump is disposed vertically in the second chamber such that the rotational axis of the electric pump is oriented in an up-down direction.

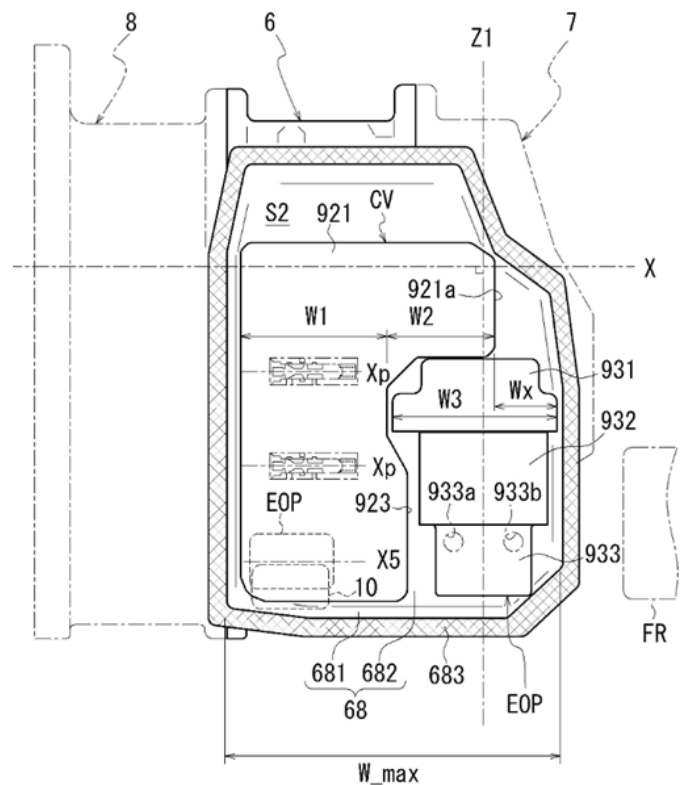


Fig. 1

発行人 (Issuer)

大 曾 根 竜 也
Tatsuya OSONE

CTO
Chief Technology Officer

編集委員会 (Editorial Committee)

編集長 (Chief Editor)

山 本 雅 弘
Masahiro YAMAMOTO

イノベーション技術開発部
Innovative Technology
Development Department

担当 (Editor)

多 田 健 一
Kenichi TADA

イノベーション技術開発部
Innovative Technology
Development Department

委員 (Members)

島 田 秀 一
Syuichi SHIMADA

技術統括部
Engineering Management Department

杉 本 正 毅
Masaki SUGIMOTO

技術統括部
Engineering Management Department

鈴 木 義 友
Yoshitomo SUZUKI

技術統括部
Engineering Management Department

道 岡 浩 文
Hirofumi MICHIOKA

開発部門
R&D Division

小 野 山 泰 一
Taiichi ONOYAMA

開発部門
R&D Division

鈴 木 勝 則
Katsunori SUZUKI

開発部門
R&D Division

荒 巻 孝
Takashi ARAMAKI

開発部門
R&D Division

梅 里 和 生
Kazuo UMESATO

開発部門
R&D Division

溝 口 裕 幸
Hiroyuki MIZOGUCHI

ジャトコ エンジニアリング (株)
部品システム開発部
Hardware System Development Department,
JATCO Engineering Ltd

谷 野 剛
Takeshi YANO

ジャトコ エンジニアリング (株)
エンジニアリングサービス部
Engineering Service Department,
JATCO Engineering Ltd

市 川 隆 義
Takayoshi ICHIKAWA

法務知財部
Legal & Intellectual Property Department

渡 邊 和 宏
Kazuhiro WATANABE

調達管理部
Purchasing Administration Department

伊 藤 洋 次
Youji ITOU

コーポレート品質保証部
Corporate Quality Assurance Department

曾 根 隆 一
Ryuichi SONE

デジタルソリューション部
Digital solution Department

中 川 季 昭
Hideaki NAKAGAWA

経営企画部
Corporate Planning Department

ジャトコ テクニカル レビュー No.24

© 禁無断転載
発行 2025 年 3 月
発行所 ジャトコ株式会社
イノベーション技術開発部
〒417-8585
静岡県富士市今泉 700-1
TEL: 0545-51-0047 (代)
FAX: 0545-51-5976
編集 有限会社 BLUE CODE
東京都世田谷区大蔵 6-14-14

JATCO Technical Review No.24

March 2025
Distributor Inovative Technology Development
Department
JATCO Ltd
700-1 Imaizumi, Fuji City, Shizuoka
417-8585, Japan

Copyrights of all articles described in this Review
have been preserved by JATCO Ltd. For permission to
reproduce articles in quantity or for use in other print
material, contact the editors of the Editorial Committee.

JATCO Ltd

700-1, Imaizumi, Fuji City, Shizuoka 417-8585, Japan

TEL: +81-545-51-0047 FAX: +81-545-51-5976

www.jatco.co.jp/english